

2012

Synthesis of fluorescent poly(styrene sulfonate)

Wayne Alfred Huberty

Louisiana State University and Agricultural and Mechanical College, whuber3@lsu.edu

Follow this and additional works at: https://digitalcommons.lsu.edu/gradschool_theses



Part of the [Chemistry Commons](#)

Recommended Citation

Huberty, Wayne Alfred, "Synthesis of fluorescent poly(styrene sulfonate)" (2012). *LSU Master's Theses*. 2587.
https://digitalcommons.lsu.edu/gradschool_theses/2587

This Thesis is brought to you for free and open access by the Graduate School at LSU Digital Commons. It has been accepted for inclusion in LSU Master's Theses by an authorized graduate school editor of LSU Digital Commons. For more information, please contact gradetd@lsu.edu.

SYNTHESIS OF FLUORESCENT POLY(STYRENE SULFONATE)

A Thesis

Submitted to the Graduate Faculty of the
Louisiana State University and
Agricultural and Mechanical College
in partial fulfillment of the
requirements for the degree of
Master of Science

in

The Department of Chemistry

by
Wayne Huberty
B.S, University of Wisconsin-Stevens Point, 2009
May, 2012

Acknowledgements

First, I would like to thank my parents for their support throughout my education and my wife for allowing us to move across country. Thanks to Dr. Paul Russo and Dr. Donghui Zhang, my research advisors, for patiently teaching me the same things over and over. To Russo group, Zhang group, Pojman group, Dr. Rafael Cueto, Dr. Sreelatha Balamurugan, and my undergraduate advisor Dr. Droske, a very gracious thank you for taking the time to help me with questions and problems.

Table of Contents

Acknowledgements	ii
Abstract.....	iv
Chapter 1 – Introduction	1
1.1 Polyelectrolytes	1
1.2 Polymer Conformation	2
Chapter 2 – Light Scattering	7
2.1 Light Scattering of Single Gas Molecule	7
2.2 Osmotic Pressure.....	12
2.4 Scattering by Large Molecules.....	15
2.5 Dynamic Light Scattering.....	17
2.6 Advantages and Disadvantages of Light Scattering	20
Chapter 3 Diffusion of Polyelectrolytes	22
3.1 Differences Between Fast and Slow Mode Diffusion	22
3.2 Models for Slow Mode Diffusion	24
Chapter 4 Fluorescence Photobleaching Recovery.....	29
4.1 Fluorescent Studies of Polyelectrolytes	29
4.2 Experimental Background	30
Chapter 5 Polystyrene Sulfonate	35
5.1 Experimental.....	35
5.1.1 Materials.....	35
5.1.2 Synthesis of FITC-labeled Vinylaniline.....	35
5.1.3 Synthesis of FITC-labeled Polystyrene Sulfonate Sodium Salt.....	36
5.1.4 Synthesis of Polystyrene Sulfonate.....	37
5.2 Characterization.....	37
5.3 Results and Discussion	38
5.3.1. FITC-Labeled Vinyl Aniline.....	38
5.3.2 Unlabeled Polystyrene Sulfonate.....	39
5.3.3 Fluorescent Polystyrene Sulfonate	41
5.3.4 Possible Causes of Unpredictable Molecular Weight.....	45
5.4 Conclusions	47
References	48
Appendix A: Permissions	52
Appendix B: List of Abbreviations and Symbols.....	61
Vita	64

Abstract

In 1978, Lee found an increase and then a large decrease in the diffusion coefficient of poly(lysine) as the concentration of salt is decreased (Lin, S. C.; Lee, W. I.; Schurr, J. M. *Biopolymers* **1978**, 17, (4), 1041-1064). Since the “slow mode” discovery, many have studied it without finding a fully satisfactory answer. Additional dynamic light scattering (DLS) measurements have been the main experimental technique used for reinvestigating the slow mode decay. Although DLS is a powerful characterization tool, it depends on thermodynamic interactions. As complicated as they can be, thermodynamic interactions are much worse for polyelectrolytes because of the charges on the polymer. This creates a difficult predicament for slow mode decay study: the slow mode decay was first discovered using DLS but DLS is not the best way to study it. Another problem with polyelectrolytes is weak scattering. Other problems associated with a DLS experiment are the tedious cleaning needed to remove dust prior to measurements, and the long acquisition times needed for a weak scatter. Therefore, other techniques are needed for the study of the slow mode decay.

Polystyrene sulfonate (NaPSS) is a commonly studied polyelectrolyte but it is not ideal. In efforts to keep the polydispersity low, NaPSS is synthesized by anionic polymerization with sulfonate groups added after synthesis of the polymer. This may allow hydrophobic patches along the polymer and could lead to aggregation in aqueous solutions, further convoluting the study of the slow mode decay. Herein, an essentially 100 % sulfonated fluorescent NaPSS is synthesized, allowing for study by fluorescence photobleaching recovery (FPR) without the possibility for “false” aggregation by the hydrophobic patches.

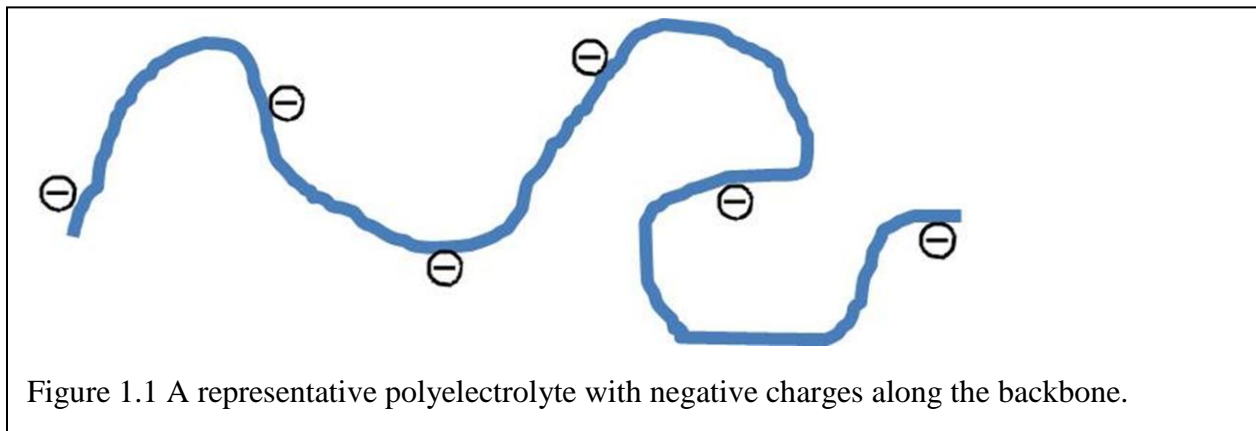
FPR has advantages for studying the slow mode decay compared to DLS. In a FPR experiment, the thermodynamic interactions are so small they can be ignored. DLS depends on

the thermodynamics of the solution; by using FPR, the slow mode problem can be made simpler (although it still is not easy). Also, the distance scale probed can be longer, thus ignoring internal motions and rotational dynamics. The amount of time needed to run a FPR experiment is much less than DLS and dust is advantageous rather than a nuisance.

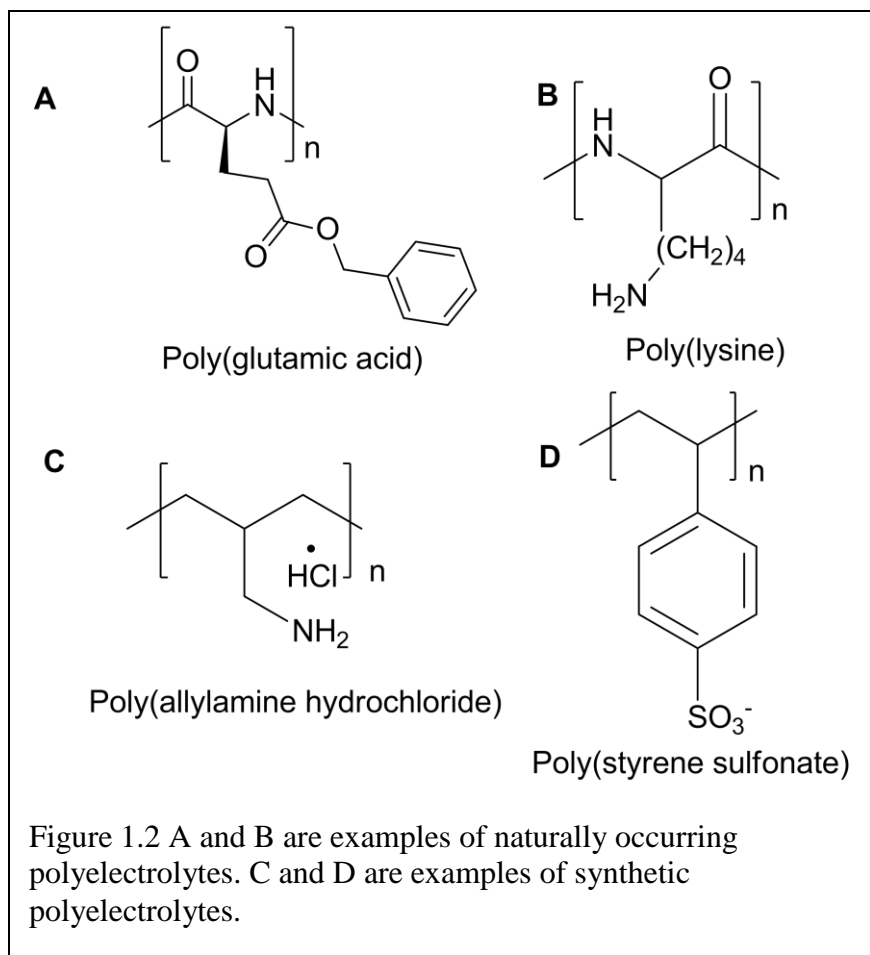
Chapter 1 – Introduction

1.1 Polyelectrolytes

Polyelectrolytes are ubiquitous, being used in a wide range of applications: from rough industrial service to flocculate colloidal matter in waste streams to elegant memory storage in all living things. As such, they have a wide versatility. Polyelectrolytes are so named due to their chemical structure, more specifically, the many charges along the polymer backbone (Figure 1.1). Figure 1.2 shows examples of natural and synthetic polyelectrolytes. Depending upon the pH of the system, the backbone of the polymer chain will be charged. Further, there are strong polyelectrolytes, e.g. polymers containing strong acid side groups, and weak polyelectrolytes, polymers containing weak acid side chains.



The charged backbone allows for several different applications for polyelectrolytes: layer-by-layer deposition onto surfaces,³ antibacterial surfaces,³ capsules,⁴ self-healing,⁵ pH sensors,⁵ protein purification,⁶ transistors,⁷ etc. Along with this assortment of applications, the charges on the polymer backbone can give the polymer an extended conformation in solution, acting as a pseudo-rod like polymer.⁸



1.2 Polymer Conformation

For each bond three different conformations are possible: trans, gauche plus, and gauche minus. Polymers are unique because they are large molecules with many different conformations. Assuming a polymer of 100 repeat units, a relatively short polymer, the total number of different conformations would be 3^{100} or 5×10^{47} . This is a tremendous number which leads to many different possible sizes and shapes. Polymer chemists attempt to classify the size in several different ways, with the first classification assuming all the backbone bonds are in the trans conformation, leading to the full contour length⁹

$$L = n \cdot l \quad \text{Equation 1.1}$$

where n is the number of bonds in the polymer backbone and l is the bond length of the backbone bonds. An example for polyethylene is as follows: assuming a molecular weight of 280,000, the number of monomer units is 10,000, so the number of C-C bonds along the backbone is 20,000. With the approximate length of a C-C bond being 1.5 Å, the contour length, L , would be $20,000 \cdot 1.5 \text{ Å} \cdot \sin\left(\frac{109.5}{2}\right) = 2,449 \text{ nm}$.⁹ Although this conformation is a possibility, it is statistically unlikely that all the C-C bonds will be in the trans conformation, so there is another way to categorize the size of a polymer, the freely jointed model. This model assumes the polymer can have any bond angle, even 180°, which cannot happen. Despite this downfall, the freely jointed model is still a valuable tool in polymer chemistry. Skipping the

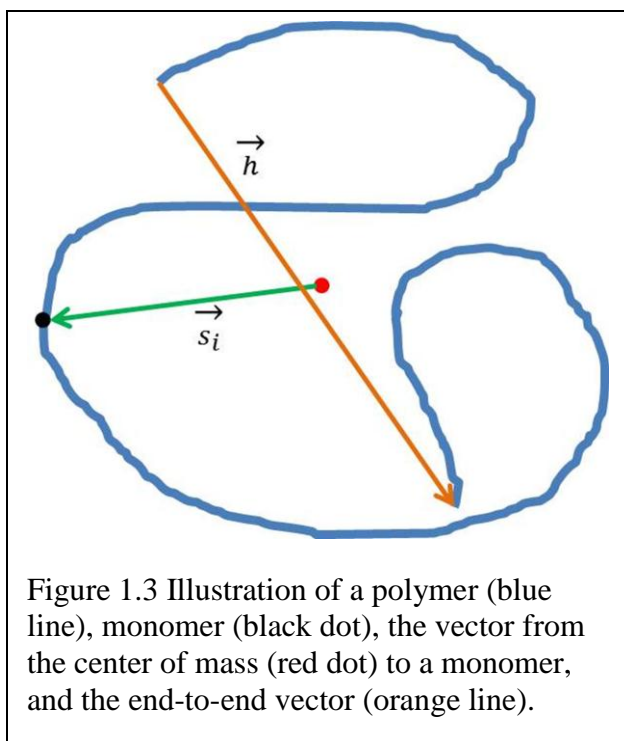


Figure 1.3 Illustration of a polymer (blue line), monomer (black dot), the vector from the center of mass (red dot) to a monomer, and the end-to-end vector (orange line).

actual derivation (see reference 6 for the full derivation), the freely jointed model says

$$\langle h^2 \rangle = n \cdot l^2 \quad \text{Equation 1.2}$$

This model provides a more representative length. For polymers, size is more meaningful than length.

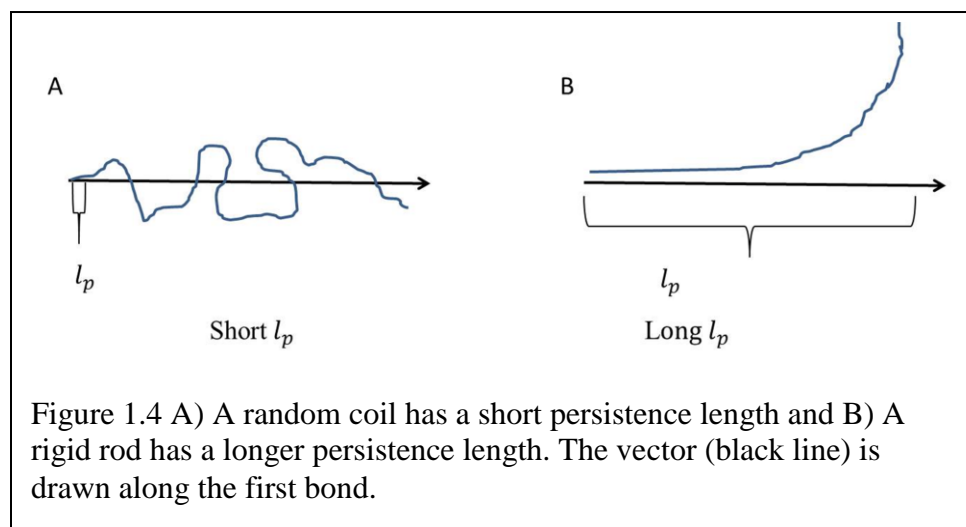
A heavily used size calculation, the root mean squared radius of gyration (R_g), is the average, mass-weighted distance of each

monomer from the center of mass of the polymer (Equation. 1.3). The polymer is not actually gyrating or rotating about an axis, this is just a lapse in polymer chemists' naming skills. Figure 1.3 illustrates the center of mass and a vector connecting it to a monomer.⁹

$$R_g^2 = \frac{\sum_{i=1}^N m_i \langle s_i^2 \rangle}{\sum_i^N m_i} \quad \text{Equation 1.3}$$

Where $\langle s_i^2 \rangle = \langle \vec{s}_i \cdot \vec{s}_i \rangle$, m_i is the mass of each monomer unit, and N is the number of monomers.⁹ The radius of gyration is a size more representative of the true size of the polymer. One last sizing scheme, further explored in Chapter 2, is R_h , the hydrodynamic radius.

Along with size, polymers have unique terms. The first discussed is persistence length, l_p which is the net projection of a hypothetical infinite chain along a tangent line drawn from the first bond of a polymer (Figure 1.4). The persistence length gives an indication of the polymer stiffness. Rigid rod polymers will have a long persistence length and random coil polymers have a shorter one. Because polyelectrolytes can be either a semirigid rod, random coil, or somewhere in between, persistence length is a valuable tool.



Two other useful measurements for polyelectrolytes are the Bjerrum length and the Debye length. The Bjerrum length is the separation distance at which two charges that have an interaction energy of $k_B T$ (Equation. 1.4). A personification of this would be “how close in proximity can two enemies get before they will separate”. Assuming the dielectric constant (ϵ)

of water is 78 and the charge of an electron is $e = 4.8 \times 10^{-10} \text{ esu}$, the Bjerrum length is 7 \AA at 298 K.¹⁰ At this length, two charges will have an energy equal to $k_B T$.¹⁰

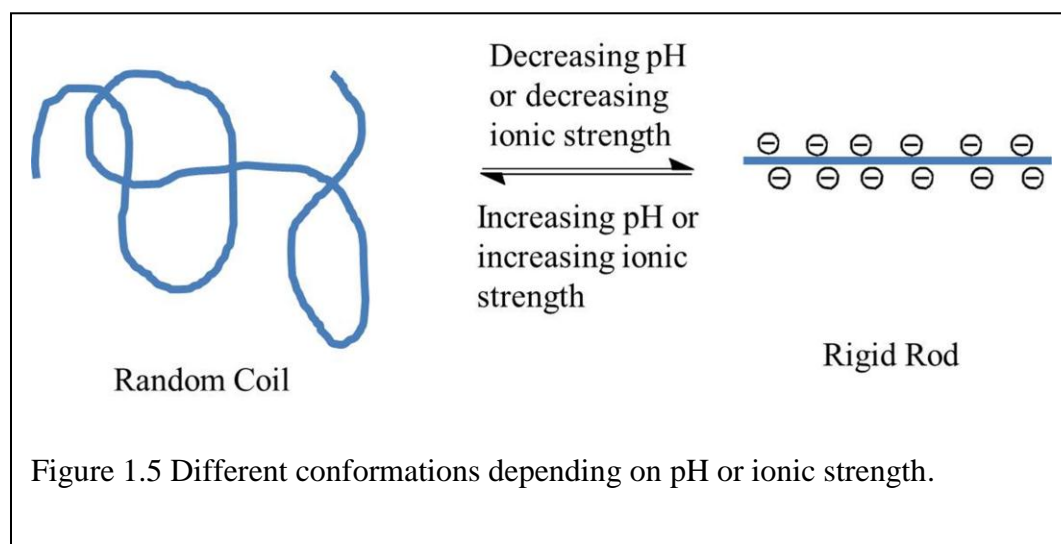
$$B \text{ in cm} = \frac{e^2}{\epsilon k_B T} \quad \text{Equation 1.4}$$

This is significant for polyelectrolytes because the Bjerrum length can be longer than the actual separation between charges along the backbone; for example, this pertains to polystyrene sulfonate where the charges can be separated by less than the Bjerrum length. When this happens, the system will rectify the problem by finding a charge somewhere and placing it near the chain to reduce the strong interactions.

The Debye length is a measure of how far apart two charges can be and yet “feel” each other’s presence

$$\kappa^{-1} \text{ in cm} = \left(\frac{8\pi N_a I B}{1000} \right)^{-1/2} \quad \text{Equation 1.5}$$

where I is the ionic strength of the solution in $\text{mol}\cdot\text{L}^{-1}$, B is the Bjerrum length in cm, and N_a is Avogadro’s number.¹⁰ A convenient mnemonic for Debye length in aqueous solutions is $1 \text{ M} = 3 \text{ Angstroms}$.



This is the first mention of ionic strength, which plays a crucial role in the size of polyelectrolytes. Depending on the concentration of salt in the solution, the charges along the backbone will be screened, allowing for the conformation to change. This is also true of changes in pH (Figure 1.5). Thus, whenever discussing polyelectrolytes, it is imperative that the ionic strength and pH are known.

Chapter 2 – Light Scattering

2.1 Light Scattering of Single Gas Molecule

Light scattering is used in such a wide range of polymer problems that it must be understood properly. Only then will it be evident why light scattering was *not* chosen as the main tool for this research.

The following developments have been adapted from Gabriel and Johnson Ch. 2.¹¹ An electromagnetic wave is a combination of oscillating orthogonal electric and magnetic fields. In scattering, the magnetic field can be ignored because the electric field is indirectly measured. In

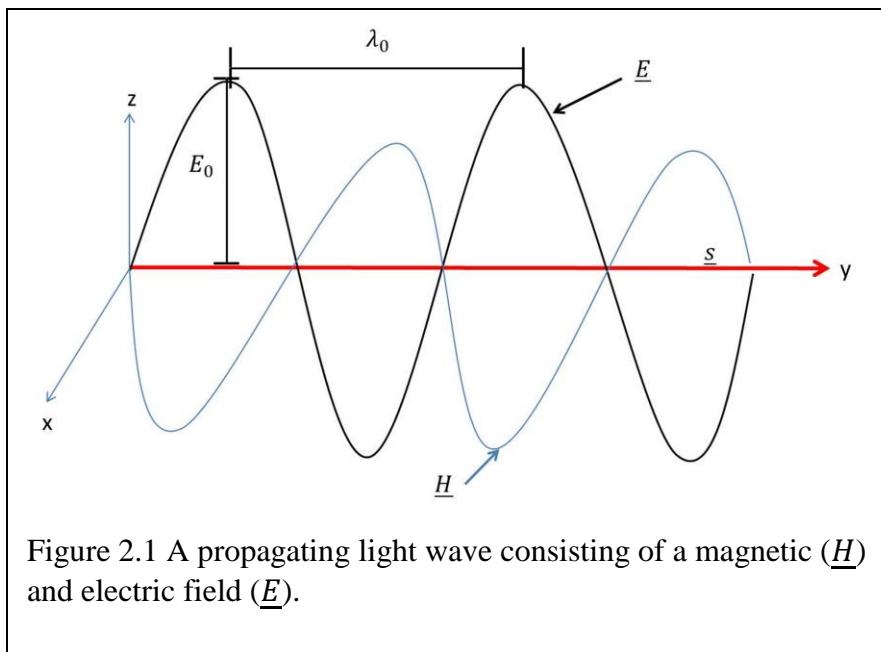


Figure 2.1 A propagating light wave consisting of a magnetic (\underline{H}) and electric field (\underline{E}).

Figure 2.1 \underline{E} is the electric field, \underline{H} is the magnetic field, λ_0 is the wavelength, E_0 is the amplitude of the electric field, and the dark red line is the direction of travel \underline{s} , which is found by the cross product of $\underline{E} \times \underline{H}$. Also, in modern

scattering experiments, a polarized wave is used and usually supplied by a laser. The polarized electric field can be described as

$$\underline{E} = E_0 e^{i(\omega t - ky)} \quad \text{Equation 2.1}$$

where k is known as the spatial frequency $k = 2\pi/\lambda_0$, λ_0 is the wavelength in vacuum, and $\omega = 2\pi c/\lambda_0$ is the laser frequency.

When molecules are bombarded with polarized light as described above, an induced dipole is created. The incident light has a high frequency ($\sim 10^{14}$ Hz for visible light) and this causes the electrons to oscillate up and down, causing the induced dipole. The nuclei are essentially not oscillating at these frequencies because protons are $\sim 1,800$ times heavier than electrons. Once created, the induced dipole emits electromagnetic radiation. A depiction of a scattering experiment is found in Figure 2.2 where θ is the scattering angle, and r is the distance from the scatterer to the detector. The oscillating dipole (the red line) can be described by Equation. 2.2 where α is the polarizability.

$$\underline{\mu} = \alpha \underline{E}_i \quad \text{Equation 2.2}$$

Oscillating dipoles create new scattered electric fields. Now, measurement of the scattered electric field needs to be developed. The proceeding equations are valid for single gas molecules but an extension to polymers will follow. The incident electric field (Equation. 2.1) leads to Equations 2.3 and 2.4. For a more thorough explanation see Gabriel and Johnson page 5.¹¹

$$\underline{E}_s = \hat{n}_s \frac{1}{rc^2} \frac{d\mu^2}{dt^2} = \frac{d^2}{dt^2} [\alpha E_0 e^{i(\omega t - \underline{k} \cdot \underline{r})}] \sin \theta_1 \frac{\hat{n}_s}{rc^2} \quad \text{Equation 2.3}$$

$$\underline{E}_s = \frac{\hat{n}_s}{rc^2} [\alpha E_0 (-\omega^2) e^{i(\omega t - \underline{k} \cdot \underline{r})} \sin \theta_1] \quad \text{Equation 2.4}$$

\hat{n}_s is the unit vector of the electric field, θ_1 is the angle between the vertical axis and the scattering vector, r is the distance from the detector, $\frac{d\mu^2}{dt^2}$ is the acceleration of the charge, and c^2 is the speed of light. Because detectors, e.g. photomultiplier tubes, do not actually measure the

electric field but the intensity, Equation. 2.5 is a way to calculate intensity from the scattered electric field given in Equation. 2.4.

$$I_s = \underline{E_s}^* \cdot \underline{E_s} \quad \text{Equation 2.5}$$

$\underline{E_s}^*$ is the complex conjugate of the electric field. Plugging Equation 2.4 into 2.5 gives

$$I_s = \frac{1}{r^2 c^4} \alpha^2 E_0^2 \omega^4 \sin^2 \theta_1 \quad \text{Equation 2.6}$$

with $\omega = \frac{2\pi c}{\lambda_0}$. Substituting $\left(\frac{\omega}{c}\right)^4 = \left(\frac{2\pi}{\lambda_0}\right)^4 = \left(\frac{16\pi^4}{\lambda_0^4}\right)$ and $E_0^2 = I_0$, giving

$$\frac{I_s}{I_0} = \frac{\alpha^2}{r^2} \left(\frac{16\pi^4}{\lambda_0^4}\right) \sin^2 \theta_1 \quad \text{Equation 2.7}$$

The point of Equations 2.3 to 2.6 is to get to Equation 2.7 and its practical applications. For example, this equation explains why the sky appears as different colors (λ_0 is in the denominator so blue light has preferential scattering power).

Equation 2.7 gives us qualitative ideas about scattering but it has difficult parameters to measure, e.g. polarizability. In order to make Equation 2.7 easier to use, we will substitute polarizability with the change of refractive index with respect to change of concentration, dn/dc . Before this, we need to return to introductory physics, particularly capacitance which is the measure of how much charge can be stored between two parallel plates.

$$\frac{C}{C_0} = \epsilon_r \quad \text{Equation 2.8}$$

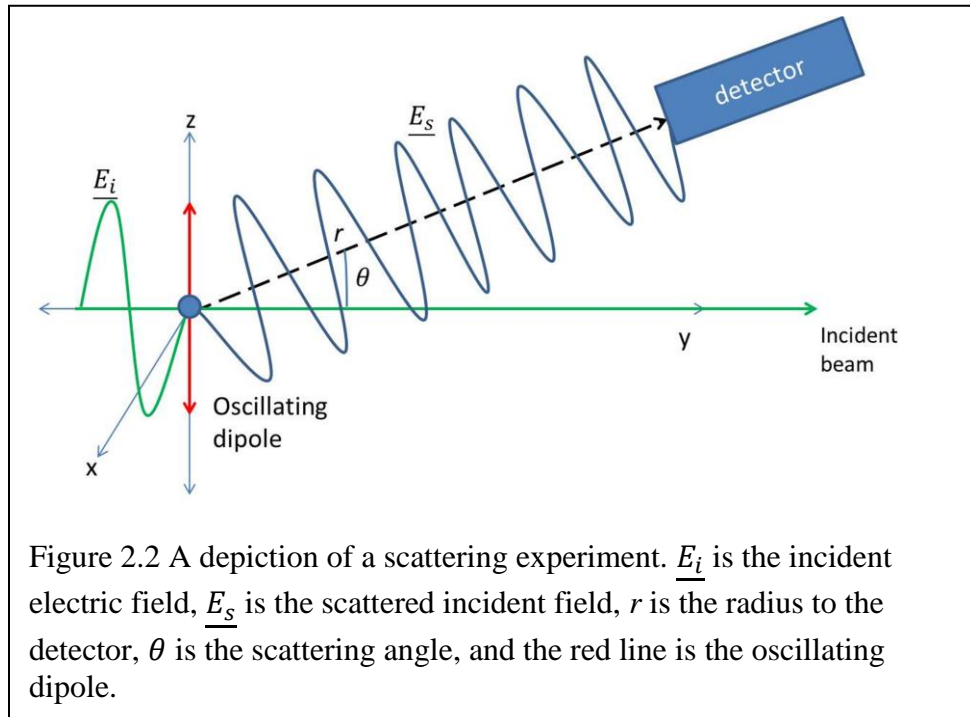
C is the capacitance measured, C_0 is the capacitance in vacuum and ϵ_r is the dielectric constant of the insulator. This is pertinent because $\lim_{\omega \rightarrow \infty} \epsilon_r = n^2$ where ω is the frequency and n is the

refractive index; the frequency of light approximately satisfies the infinite limit. This means the capacitance can be measured for visible light by measuring the refractive index. To correlate refractive index and polarizability (refractive index is easier to practically use) we use the Debye Relation to give Equations 2.9 and 2.10.

$$n^2 = 4\pi v\alpha \quad \text{Equation 2.9}$$

where v is the number density and

$$n^2 - 1 \cong 2 \left(\frac{dn}{dc} \right) c \quad \text{Equation 2.10}$$



Combining Equations 2.9 and 2.10

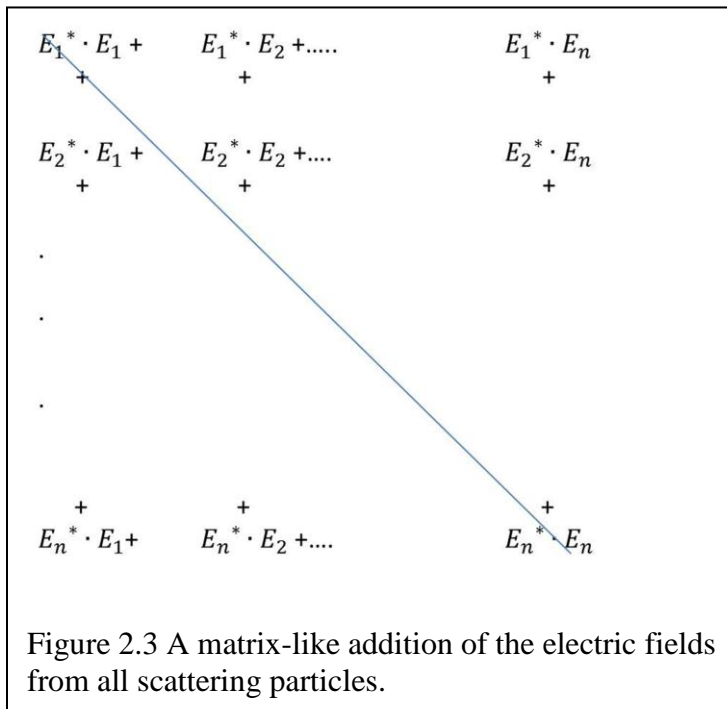
$$\alpha = \frac{2c \left(\frac{dn}{dc} \right)}{4\pi v} \quad \text{Equation 2.11}$$

where number density, $v = \frac{cN_A}{M}$, c is the concentration and M is the molecular weight.

Substituting polarizability (Equation 2.11) into Equation 2.7,

$$\frac{I_s}{I_0} = \frac{4\pi^2}{\lambda_0^4 r^2} \left(\frac{M}{N_A}\right)^2 \left(\frac{dn}{dc}\right)^2 \sin^2 \theta_1 \quad \text{Equation 2.12}$$

This provides an equation that is valid for one gas particle and eliminates polarizability, replacing it with the change in refractive index with respect to concentration. The dn/dc is much easier to measure than polarizability and in the process the equation now allows the molecular weight to be found.



For a single gas particle it was developed that an oscillating dipole will release electromagnetic energy and the electric field is detected. For many gas particles the electric field at the detector will be an addition of the electric fields from each scatterer. The sum of these contributions is conveniently arranged in a matrix-like form (Figure 2.3). Lining up each

addition into this pseudo-matrix allows us to see what happens: all the non-diagonal terms will cancel because of their phase difference.¹² Modifying Equation 2.12 by dividing both sides by the scattering volume and concentration, $c = \frac{n \cdot MW}{N_A \cdot Volume}$,

$$\left(\frac{1}{V}\right) \frac{I_s}{I_0} = \frac{2\pi^2 c M \left(\frac{dn}{dc}\right)^2}{\lambda_0^4 r^2 N_A} G \quad \text{Equation 2.13}$$

For polarized light, $G = 2\sin^2 \theta_1$ and for unpolarized light $G = 1 + \cos^2 \theta_1$. Equation 2.13 shows $I_s \propto \text{concentration} \cdot M = n \cdot M^2$. In order to have intense scattering, there must be enough particles to scatter (concentration) or the particles must have a large molecular weight (polymers). This also shows the importance of clean cells for light scattering. Dust is huge compared to the analyte in solution; this is the kiss of death trying to

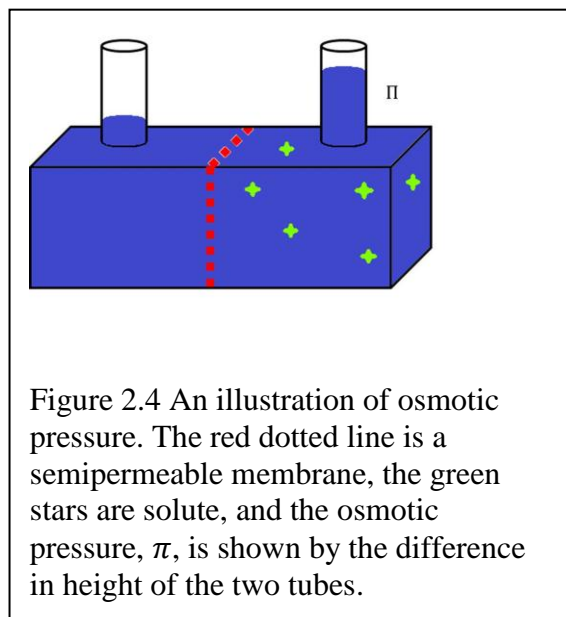


Figure 2.4 An illustration of osmotic pressure. The red dotted line is a semipermeable membrane, the green stars are solute, and the osmotic pressure, π , is shown by the difference in height of the two tubes.

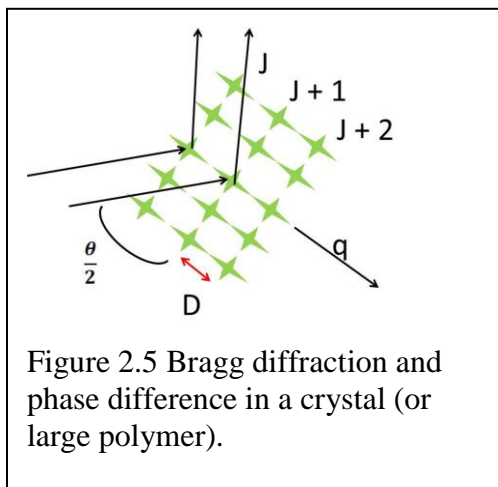
detect scattering of polymers because the scattering intensity is proportionate to radius to the sixth power (this happens because $M \sim R^3$)!

2.2 Osmotic Pressure

Scattering is a number and size game according to Equation 2.13: the more particles and the larger they are, the more intense the scattering. While this is true for point particles, there is no such thing. Once finite size is considered, larger does not always produce more scattering.

Because scattering is partly based on the number of scatterers, it is intricately tied to colligative properties. In an experiment to measure osmotic pressure a semipermeable membrane

separates a solution and a pure solvent. The pure solvent will cross the membrane and increase the volume of the solution. The associated pressure is known as the osmotic pressure (Figure 2.4),^{13, 14}



$$\Pi = MRT \quad \text{Equation 2.14}$$

where Π is the osmotic pressure, M is the molarity, R is the gas constant, and T is temperature. Osmotic pressure can be easily measured by the difference in height between the two tubes in Figure 2.4. Another way to find osmotic pressure is by chemical potential and this feature is important to the development for

light scattering (see Equation 2.18).

2.3 Scattering due to Concentration Fluctuations

The intensity of scattering was shown to depend on the number of scatterers and their molecular weight. Scattering is caused by oscillating dipoles, but concentration fluctuations in the solution allow the scattered light to be detected. Without these concentration fluctuations, the scattering would be like that of a pure solution, essentially zero. All particles will scatter light, but there will be destructive interference unless the particles are a certain distance apart (D) on the order of the distance between atoms. This is known as Bragg scattering.⁹ In a perfect crystal, each scatterer will be equidistant from every other and no scattering is possible because total destructive interference occurs except at certain angles which satisfy the Bragg condition. Once an imperfection is placed in the crystal lattice, some scattered light will have constructive interference and can be detected. To correlate imperfections in a crystal lattice to concentration

fluctuations, the fluctuations can be understood as “imperfections” that allow for some of the scattered light to be detected. To quantify the changes in concentration, the average is taken and is inserted into Equation 2.13 to give

$$\left(\frac{1}{V}\right) \frac{I_s}{I_0} \propto \frac{\left(\frac{dn}{dc}\right)^2 \overline{(\partial c)^2}}{\lambda_0^4 r^2} \quad \text{Equation 2.15}$$

where once again polarizability has been exchanged in favor of dn/dc . In order to find the mean-squared concentration fluctuations, $\overline{(\partial c)^2}$. Boltzmann’s law is used

$$P(\partial c) = e^{\left(\frac{-\Delta G(\partial c)}{k_b T}\right)} \quad \text{Equation 2.16}$$

After integration to find the mean-squared fluctuation at constant temperature and pressure,

$$\overline{(\partial c)^2} = \frac{k_b T}{\left(\frac{\partial^2 G}{\partial c^2}\right)_{c=c'}} \quad \text{Equation 2.17}$$

Equation 2.17 says that the concentration fluctuations are described by the ratio of thermal energy to the second derivative of the Gibbs energy. Because chemical potential is analogous to the second derivative of the Gibbs energy, it can be substituted into Equation 2.15 to give

$$\left(\frac{1}{V}\right) \frac{I_s}{I_0} = \frac{2\pi^2 n_0^2 \left(\frac{dn}{dc}\right)^2}{\lambda_0^4 r^2} \left[\frac{c}{\left(\frac{-1}{k_b T \bar{v}_1}\right) \left(\frac{\partial \mu_1}{\partial c}\right)} \right] 2 \sin^2 \theta_1 \quad \text{Equation 2.18}$$

where n_0 is the refractive index of the solvent, \bar{v}_1 is the partial molar volume of the solvent, and μ_1 is the chemical potential of the solvent. Because osmotic pressure and chemical potential are related, osmotic pressure can be inserted into the equation in place of chemical potential.

$$\left(\frac{1}{V}\right) \frac{I_s}{I_0} = \frac{2\pi^2 n_0^2 \left(\frac{dn}{dc}\right)^2}{N_A \lambda_0^4 r^2} \left[\frac{c}{\left(\frac{1}{RT}\right) \left(\frac{\partial \pi}{\partial c}\right)} \right] 2 \sin^2 \theta_1 \quad \text{Equation 2.19}$$

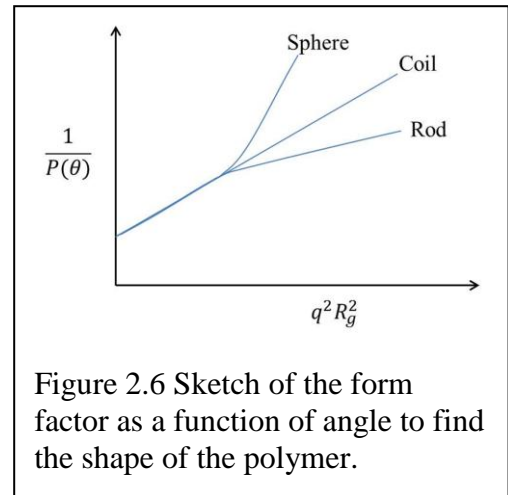
This equation is important because it states that the scattering is inversely related to $\frac{\partial \pi}{\partial c}$, the osmotic stiffness, which is a thermodynamic term. This means that light scattering relies on the thermodynamic interactions between the solvent and solute. This can create problems for samples where the thermodynamic interactions are complicated, e.g. polyelectrolytes. A virial expansion of the $\frac{d\pi}{dc}$ term gives

$$\left(\frac{1}{V}\right) \frac{I_s}{I_0} = \frac{2\pi^2 n_0^2 \left(\frac{dn}{dc}\right)^2}{N_A \lambda_0^4 r^2} \left[\frac{c}{N_A \left(\frac{1}{M} + 2A_2 c + 3A_3 c^2 + \dots\right)} \right] 2 \sin^2 \theta_1 \quad \text{Equation 2.20}$$

To plot Equation 2.20, the Rayleigh ratio (\mathcal{R}) and optical constant (K) are used. The Rayleigh ratio (more properly called a factor because it has units) is effectively the excess scattered light per unit volume per unit radian; in other words, is the scattering intensity greater than the solvent scattering intensity (a baseline correction). The optical constant, K , is found in Equation 2.21.

$$K = \frac{4\pi^2 n_0^2 \left(\frac{dn}{dc}\right)^2}{\lambda_0^4 N_A} \quad \text{Equation 2.21}$$

Plotting $\frac{Kc}{\mathcal{R}} = \frac{1}{M} + 2A_2 c^2 + 3A_3 c^3 + \dots$ gives the y-intercept as the inverse of the molecular weight and the slope as second virial coefficient.



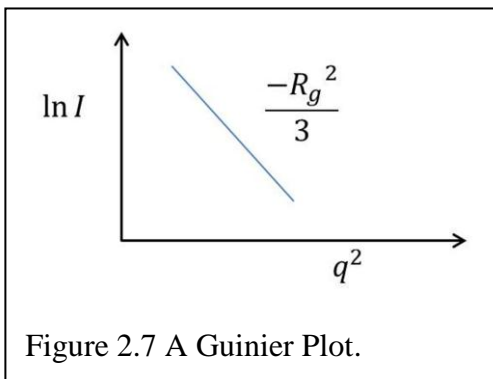
2.4 Scattering by Large Molecules

The proceeding developments for scattering have all assumed a small molecule. What happens when the molecule is large and there exists a possibility for monomers along the polymer chain are far enough apart to cause destructive interference in the scattering intensity? It

will be assumed that the refractive index of the large polymer is homogenous and the Rayleigh-Debye limit, $4\pi L(\Delta n) \sin(\theta/2)/\lambda \ll 1$, is satisfied. L is the largest dimension of the particle and Δn is the difference in refractive index between the polymer and the solvent. Bragg's law can be used to explain how the intensity will be modulated at different angles and it defines the scattering vector, q .

$$q = \frac{4\pi n}{\lambda_0} \sin\left(\frac{\theta}{2}\right) \quad \text{Equation 2.22}$$

Because of the angular dependence of the scattering intensity, the shape of the polymer can be determined from the form factor, $P(\theta)$. For a derivation of the form factor see Gabriel and Johnson. From a plot of $1/P(\theta)$ as a function of $q^2 R_g^2$, different slopes at high $q^2 R_g^2$ for spheres, rods, and random coils are found (Figure 2.6). Explicit form factor equations are known for many shapes and can be fit to experimental data.



The problems with the plot of the form factor are R_g needs to be known and $qR_g < 1$. Details about the shape can be inferred outside the Guinier regime at high q . To find R_g , a Guinier Plot is used (Figure 2.7) with the slope giving $-R_g^2/3$. The disadvantage of a Guinier plot is that low angles

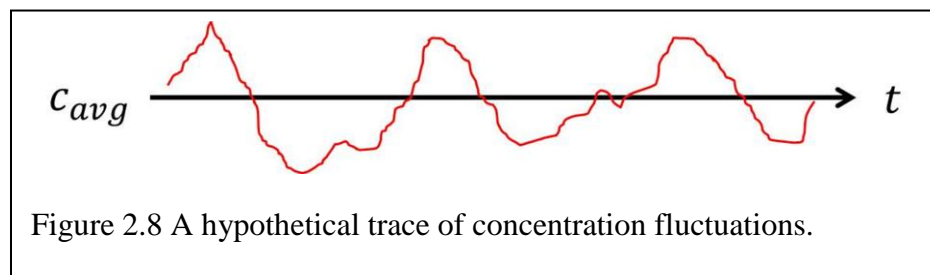
must be used and the data must be quiet. If the shape of the polymer is known beforehand, higher angles can be used and nonlinear fitting can be used to find R_g .

Thus far, equations for scattering have been semi-derived and it has been shown that scattering can be a useful tool to find absolute molecular weight and radius. Dynamic light

scattering was historically the experimental method of choice to study polyelectrolytes; however, the main focus of this research will be on fluorescence photobleaching recovery and the diffusion coefficient it provides.

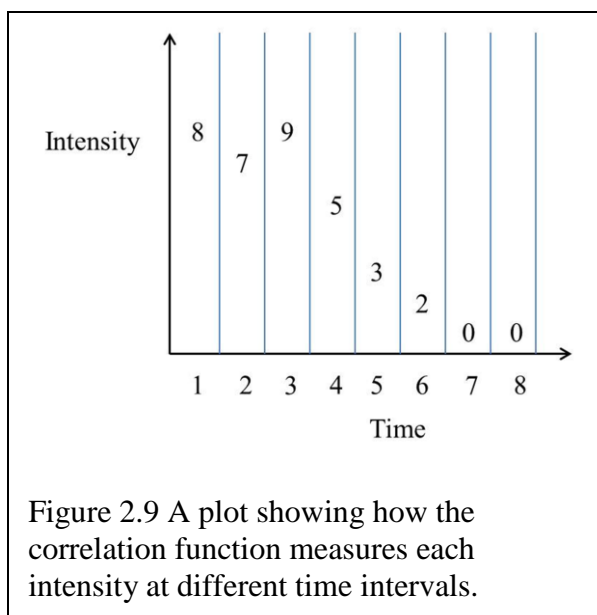
2.5 Dynamic Light Scattering

In dynamic light scattering (DLS), the change in concentration is followed, as opposed to the total scattering intensity. These changes in concentration are very small, but at small time scales (micro or even nanoseconds) the changes in concentration can be detected.



These concentration fluctuations allow scattering to be detected and their persistence in term can be described by the intensity autocorrelation function.¹¹ The autocorrelation function will decay as the changes in intensity are “less correlated”.

A DLS experiment observes a large portion of the particles. During the acquisition of a correlation function, a photon counting device keeps track of the intensities measured over small time intervals. If the total intensity would be recorded by a slow detector (e.g. static light scattering) and then analyzed for changes in intensity, they would be too small to detect.



Decreasing the number of particles studied allows for greater relative changes in concentration, but if the number of particles is decreased too far the variation in the number of particles itself will contribute to the fluctuating signal. This is undesirable; what DLS must see is the fluctuations due to phase shifts as a large number of particles diffuse a distance $2\pi/q$ in the direction of the scattering vector, q . Number fluctuations introduce another source of intensity fluctuations; what is worse, the fluctuations are slow because they are associated with the dimensions of that part of the sample which the detector sees, which is normally much larger than $2\pi/q$. For the correlation function, the initial product of intensities likely has a value greater than 0, but it tends to zero as the time difference increases (Figure 2.9). The first order correlation function can be found in Equation 2.23 and a plot of the first order correlation function gives an exponential decay (Equation 2.24).

$$g^{(1)}(t) = \lim_{T \rightarrow \infty} \frac{1}{2T} \int_{-T}^T E^*(t') E(t' + t) dt'$$

Equation 2.23

$$g^{(1)}(t) = e^{-\gamma t}$$

Equation 2.24

where

$$\gamma = q^2 D$$

Equation 2.25

In Equation 2.23, the electric field is measured for the first-order correlation function; however, intensities are measured in an experiment, not electric field. Thus, the second-order correlation function (Equation 2.26) is used. The first-order correlation function is useful because of Equations 2.24 and 2.25, providing a means to find the diffusion coefficient, D . The Siegert

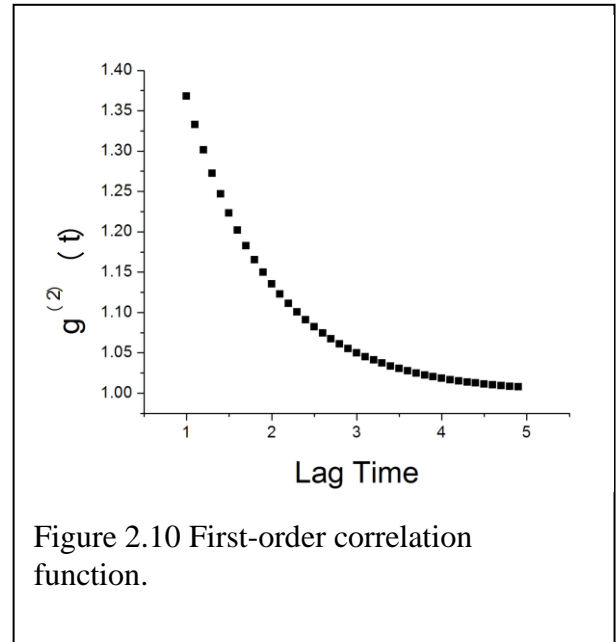


Figure 2.10 First-order correlation function.

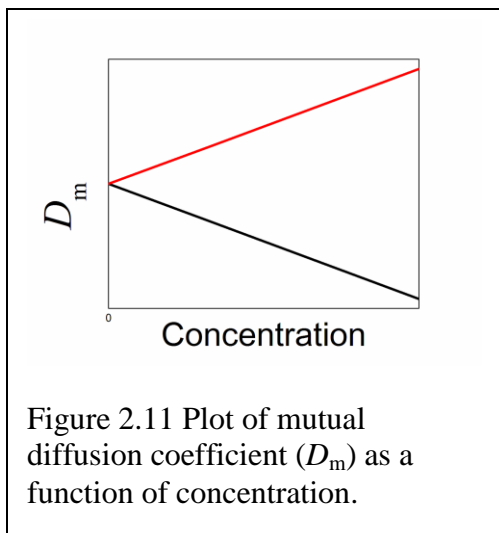
relation, a way to traverse the gap from the second order correlation function to the first, is found in Equation 2.27.¹¹

$$g^{(2)}(t) = \lim_{T \rightarrow \infty} \frac{1}{2T} \int_{-T}^T I^*(t') I(t' + t) dt' \quad \text{Equation 2.26}$$

$$g^{(2)}(t) = 1 + f(A) |g^{(1)}(t)|^2 \quad \text{Equation 2.27}$$

where $f(A)$ is the coherence parameter and can be found in Figure 2.10. The coherence parameter is chosen (mostly by optical settings) at the start of the experiment and is $0 < f(A) < 1$. If the coherence is large the signal is “noisy”—this noise is the desirable essence of the experiment—but if it is small, the signal will be quiet and useless.

All the previous discussion has been to get to this point: to understand the diffusion coefficient. The diffusion coefficient explains the movement of a molecule in solution. An easy example of diffusion is adding one drop of food coloring to a glass of water and watching the color slowly fill the cup. Some important applications of the diffusion coefficient are fuel cells and the description of hydrogen diffusion, the diffusion of carbon dioxide in carbonated beverages (try telling Coca-Cola it’s not important!), and in the case most pertinent to this research, it provides the hydrodynamic radius.^{9,15,16} There are multiple diffusion coefficients but only two are discussed: mutual diffusion coefficient D_m , optical tracer diffusion coefficient D_s .⁹ The mutual diffusion coefficient is due to concentration fluctuations and the self-diffusion coefficient is due to movement of a labeled molecule and not dependent on concentration fluctuations.



The first appearance of the diffusion coefficient is in Equations 2.24 and 2.25. Through the Stokes-Einstein relation the size can be found (Equation 2.28).

$$D_s = \frac{k_b T}{f} \quad \text{Equation 2.28}$$

where f is the friction factor. Plugging in the friction factor for a sphere into Equation 2.28 gives

$$D_0 = \frac{k_b T}{6\pi\eta_0 R} \quad \text{Equation 2.29}$$

where R is the radius of the particle and η_0 is the viscosity of the solvent.

The question remains for shapes other than spheres and the answer lies in a new term, hydrodynamic radius, R_h . The hydrodynamic radius is defined as the size of an equivalent sphere that would diffuse at the same rate as the real particle. Thus, it can be defined

$$R_h \equiv \frac{k_b T}{6\pi\eta_0 D_0} \quad \text{Equation 2.31}$$

The mutual and self-diffusion coefficients are identical at $c \rightarrow 0$ (Figure 2.11).

Beside the difference in the definition of the diffusion coefficients, they are found in different experiments. For example, mutual diffusion is found by DLS but the self-diffusion (more correctly, the optical tracer self-diffusion) is found by fluorescence photobleaching recovery (FPR), which will be discussed later.

2.6 Advantages and Disadvantages of Light Scattering

Light scattering has advantages and disadvantages. The major advantage is that the absolute molecular weight is found in static light scattering. Other techniques do provide absolute molecular weight but any technique that provides a true molecular weight is highly sought after. Second, it can give other parameters, e.g. R_g , R_h and diffusion coefficients. Besides

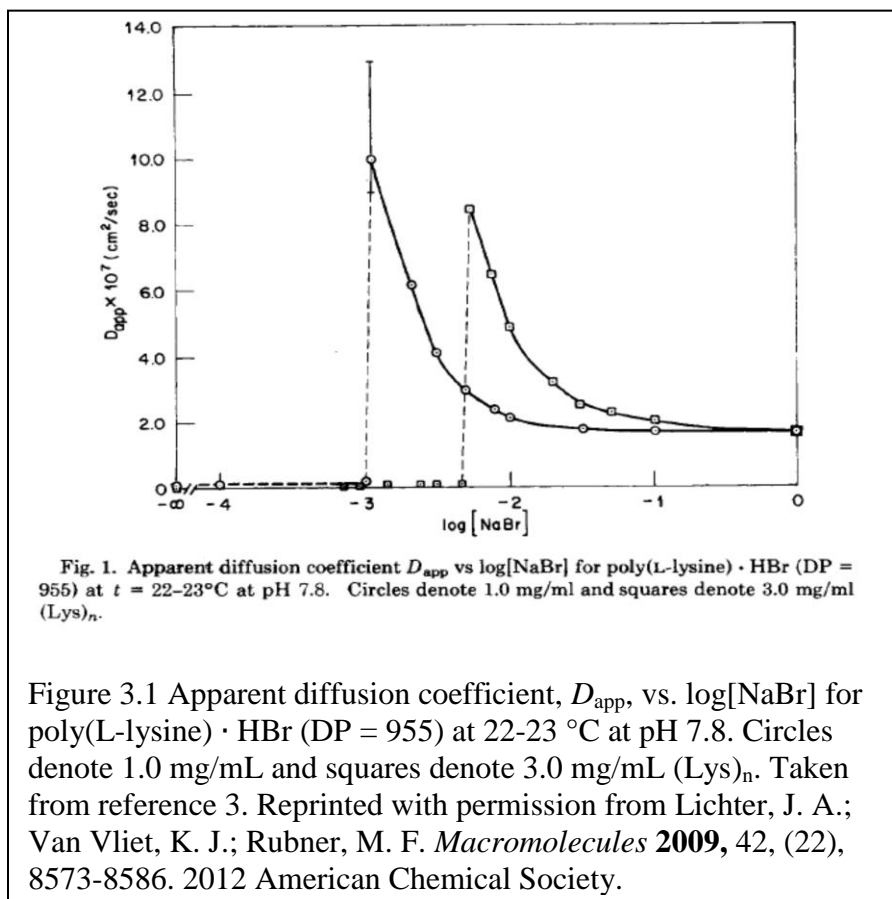
the two diffusion coefficients previously discussed, DLS can tell if a rigid rod polymer is tumbling in solution and can find aggregation.

Light scattering has many drawbacks. It struggles when there is any dust in the sample cell. The intensity is proportional to the radius of the particle to the sixth power and dust is extremely large compared to the polymer sample. This means extensive cell cleaning and filtering until the cell and solvent are clean; dust free samples are also required. Lab-synthesized polymers tend to be dusty and filtering the sample to eliminate the dust may filter the polymer as well. There is also the problem of stray light; if stray light scattered by air-glass interfaces enters the detector, it will give false data. This can be largely reduced but not completely.

The previous problems can be largely eliminated, but there is one major disadvantage for DLS of polyelectrolytes: light scattering is a thermodynamic experiment. Polyelectrolytes have complicated thermodynamics because of their charged backbone. Studies on polyelectrolytes have debated DLS results for the last 40 years and the emphasis of this research is to depart from the thermodynamic interactions and follow the self-diffusion coefficient.

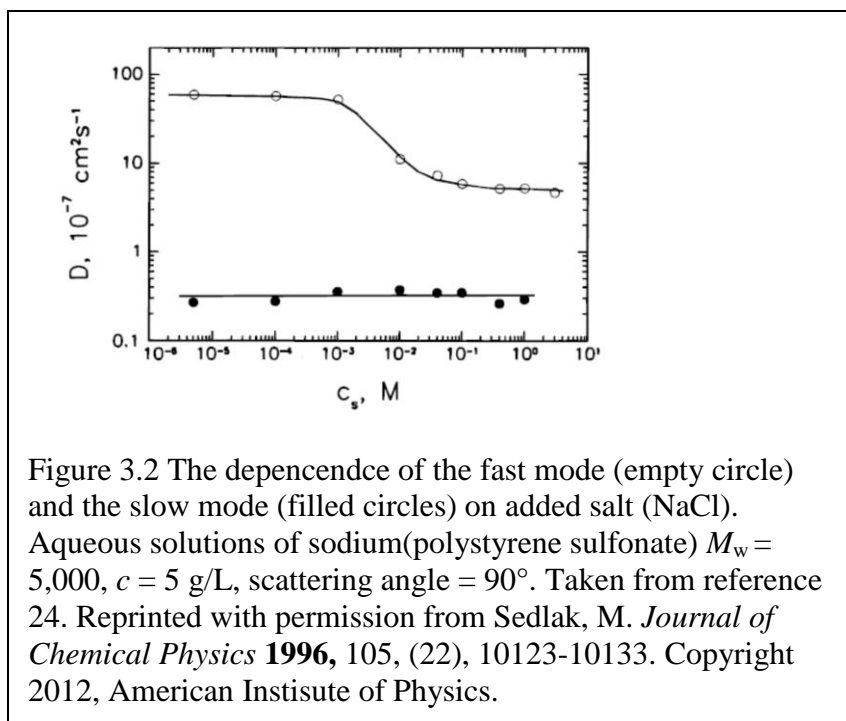
Chapter 3 Diffusion of Polyelectrolytes

3.1 Differences Between Fast and Slow Mode Diffusion



As previously discussed, polyelectrolytes have charges along the polymer. The number of charges depends on: A) the type of polymer, whether it is a strong or weak polyelectrolyte, and B) the ionic strength of the solution. These factors also affect the diffusion coefficient. Lee et al. investigated the diffusion coefficient of poly-L-Lysine as a function of added salt (Figure 3.1).^{2,17}

At decreasing salt concentrations the diffusion coefficient increases until a specific salt concentration, where the apparent diffusion coefficient dramatically declines. The region of salt concentrations higher than the sharp decline is known as the fast-mode diffusion, or the normal mode. The region of salt concentrations below the sharp decline is known as the slow-mode, or the extraordinary mode.²



After Lee et al. set the precedent for the disparity between diffusion modes, others investigated various polyelectrolytes to see if they too exhibited a drop in the diffusion. Some polyelectrolytes studied were polystyrene sulfonate,¹⁸ DNA,¹⁹ poly(2-vinylpyridine),²⁰ poly(adenylic acid),²¹ poly(methacrylic acid),²² or more recently a block copolymer of poly(p-azidomethylstyrene)-co-polystyrene.²³ It was found that for polyelectrolytes in general, there appears fast and slow mode diffusion in the range of concentration of polyelectrolyte/concentration of salt (c_p/c_s) of 1 to 5.

The fast and slow modes appear at different salt concentrations for different molecular weights, but they also have different properties depending on salt concentration, polymer concentration, and molecular weight. For Figures 3.2 the filled circles are the slow mode diffusion and the empty circles are the fast mode diffusion. Figure 3.2 shows the influence of salt on the slow and fast mode diffusion.²⁴ Staying within the slow mode regime, there is little or no dependence of the diffusion coefficient on the molecular weight. The same cannot be said for the

fast mode diffusion. Also, the fast and slow mode were investigated for the dependence of diffusion on polyion molecular weight, Figure 3.3 and Figure 3.4.¹⁸

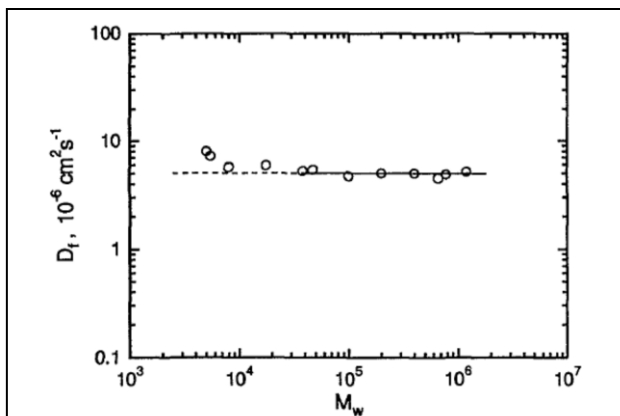


Figure 3.3 Dependence of fast diffusion coefficient on polyion molecular weight. Poly(styrene sulfonate sodium salt) in water, no added salt, polyion concentration = 45.6 g/L, scattering angle = 90°. Taken from reference 18. Sedlak, M.; Amis, E. J. *The Journal of Chemical Physics* **1992**, 96, (1), 817-825. Copyright 20120, American Institute of Physics.

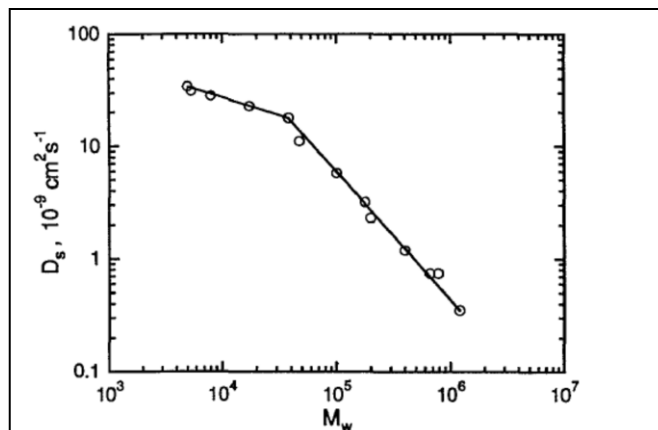


Figure 3.4 Dependence of slow diffusion coefficient on polyion concentration. Poly(styrene sulfonate sodium salt) in water, no added salt, polyion concentration = 45.6 g/L, scattering angle = 90°. Taken from reference 18. Sedlak, M.; Amis, E. J. *The Journal of Chemical Physics* **1992**, 96, (1), 817-825. Copyright 2012, American Institute of Physics.

3.2 Models for Slow Mode Diffusion

Katchalsky et al. and Lifson et al. set the basis for explaining what occurs at low salt concentration. They imagined the polyelectrolytes as semirigid rods due to the strong repulsive force between like charges at low salt concentrations.^{25,26} After Katchalsky et al., de Gennes looked at the effect of polymer concentration of polyelectrolyte solutions, finding critical concentrations.²⁷ For low polymer concentrations the polymers are too dilute to have any interaction, allowing the polymers to be at a fully extended conformation. This cannot last as the concentration increases and at a higher polyelectrolyte concentration the individual chains will have interactions with other chains and form a lattice. Continuing to add polyelectrolyte will make the chains interpenetrate and form a network. The resultant screening makes the

polyelectrolytes more flexible but there is still no contact between chains because of the like charges of the polyelectrolytes.

Right around the time of de Gennes' work on polymer conformation multiple authors developed scaling relations for polyelectrolyte solutions.²⁷⁻²⁹ Odijk found a scaling relation dependent on the electrostatic persistence length (see chapter 1.2 for a discussion of persistence length).³⁰ The total persistence length, l_t , is a sum of electrostatic persistence length, l_e , and the persistence length, l_p , and is related to the concentration by $l_t = c^{-1}$. When the total persistence length is equal to the full contour length, $l_t \cong l$, a critical concentration is reached, c^* , and different regimes can be determined (Table 3.1). c_G^* is the overlap concentration found by de Gennes.²⁷ Odijk describes the correlation length, ξ , using blob theory: each polyelectrolyte chain is a blob. The correlation length is the radius of each blob and within the blob there is no interference from other blobs. At the melt temperature, c^{**} , there is an isotropic phase where $l_t \ll \xi$. Ultimately, scaling relations can be found for the different concentration regimes: at $c^{**} > c > c^*$, $\xi \sim c^{-1/2}$ and $R \sim c^{-1/2}$. At concentration region $c > c^{**}$, $\xi \sim c^{-3/8}$ and $R \sim c^{-5/16}$.³¹

Table 3.1 Different concentration regions

Region	Concentration Range	Qualitative Remarks
A	$c_G^* \gg c$	Very dilute; negligible interaction between the polyions
B	$c^* > c > c_G^*$	Dilute/semidilute; polyions remain rigid and interact strongly
C	$c^{**} > c > c^*$	Drastic decrease in the viscosity due to large decrease in polyion dimension

These theoretical bases allowed Drifford et al.³² to explain a q -dependence in the scattering for polystyrene sulfonate sodium salt (Figure 3.5) and its scaling relation: $q \sim c^{1/2}$. They attempted to explain their results based on two theories: correlation hole and long-range Columbic interactions. A correlation hole arises when a polyion has a “shell” around itself that repels other polyions. This will cause a somewhat ordered structure in solution and cause a maximum in the scattering. The Columbic interactions are believed to be small, a few interparticle spacings, aiding the short order. They believed their data were best described by the Katchalsky theory of aligned rods.³³ As a note, Schurr and Schmitz also thought the slow mode was caused by aggregates.³⁴ Another reason is it believed the slow mode diffusion is caused by aggregates is a study by Mattice et al.³⁵ In this study, a nonradiative singlet energy transfer was performed to probe the distance scales between polymers. At low salt concentrations there was a higher efficiency of

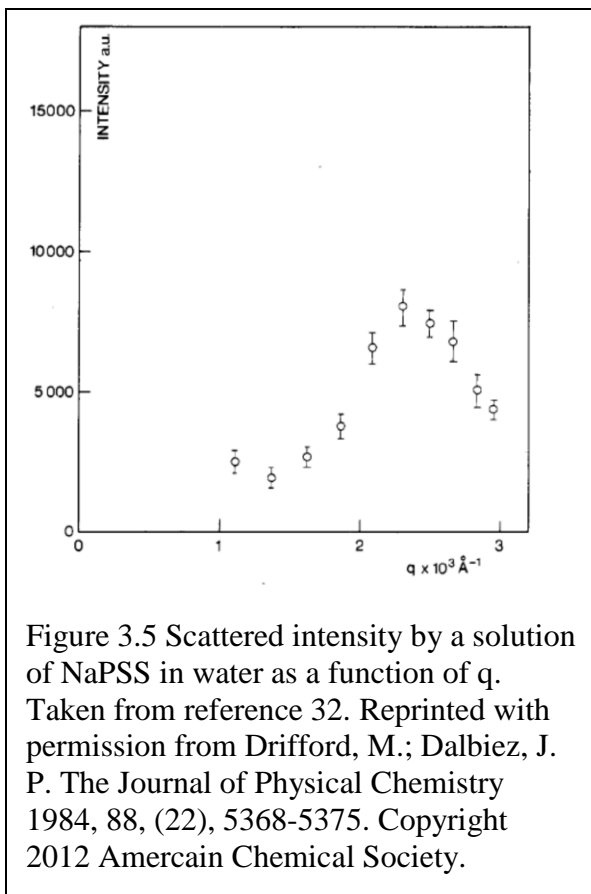


Figure 3.5 Scattered intensity by a solution of NaPSS in water as a function of q . Taken from reference 32. Reprinted with permission from Drifford, M.; Dalbiez, J. P. *The Journal of Physical Chemistry* 1984, 88, (22), 5368-5375. Copyright 2012 American Chemical Society.

the energy transfer for the largest radii (5 nm), showing there is some order present and the chains are close to each other, but not entangled.

Stigter brought another possibility for the slow mode diffusion: an isotropic-anisotropic transition.³⁶ There has been no optical evidence of this, such as birefringence, but Stigter believed the transition from coil to rod could cause this isotropic-anisotropic transition. This is

not fully agreed upon, and Schmitz states that the transition is too abrupt for it to be caused by the coil-rod transition.³⁷ Further, the coil-rod transition would depend of molecular weight and Drifford found the transition from ordinary to extraordinary phase was independent on the molecular weight; it only depended on the type of polyion used, the nature of the solvent, and the valence of the counterion.³⁸

Not only is there a peak in the dynamic light scattering, but it is present in x-ray scattering as well. Because x-ray and light scattering are very similar but probe different distance scales, it is expected to see the peak in the scattering as a function of q . Amis et al. found in small angle x-ray scattering (SAXS) the presence of a peak in the scattering.³⁹ They attribute the peak to the slow mode caused by multichain domains that were found to be 60 – 100 nm in size by static light scattering.^{18, 40} Amis says “in the spirit of Muthukumar” the multichain domains will follow his idea that there will be a weak attraction between like charges in a dilute polyelectrolyte solution.⁴⁰ Other models use regions of attractive interactions, leading to polyelectrolyte cooperation in solution.⁴¹⁻⁴⁴

A more current study by Zhang et al. used analytical ultracentrifugation (AUC) to find the diffusion coefficient of polystyrene sulfonate sodium salt.⁸ It was found that there were fast and slow mode diffusion processes occurring, just like DLS.^{8, 45} They too agree the slow mode is caused by multichain domains. Along with the diffusion coefficient, Zhang et al. found the conformation of the chain is affected by the concentration of salt. As the concentration of salt increased, the conformation went from an almost rigid rod to a random coil (corroborates previous assumptions).

Different studies can have different interpretations of possible causes for the slow mode. For example, Wu et al. studied a polymer that can reversibly become a polyelectrolyte. It showed

fast and slow modes when the polymer is a charged, but when the polymer is neutralized there is only one diffusive mode.²³ They claim the slow mode diffusion is caused by self-diffusion that is slowed by the electrostatic repulsions of other chains, but not ruling out that “cages” of aggregates could slow the self-diffusion. Zhang was a co-author with Wu but claims that the slow mode is due to multichain domains.⁸

When the literature—at least that based on NaPSS—is distilled into one sentence, it could read as the following “There exist fast and slow modes of diffusion for polyelectrolytes, but almost every study⁴⁶ performed has used an inferior polystyrene sulfonate (at least the ones using PSS)”. It is proposed in this research that an essentially 100% sulfonated polystyrene sulfonate sodium salt needs to be used to clarify the ambiguity associated with the slow mode. Using Zhang’s work as a reference, the “best” polymer was less than 93% sulfonated. This leaves aromatic side chains unsulfonated that could lead to aggregation. Studies with weak polyelectrolyte that have tunable hydrophobic character have tried to address the idea that aggregation causes the slow mode diffusion, but there were no strong polyelectrolytes synthesized.^{34,35,38,39,41,46} There exists a need for a fluorescently labeled strong polyelectrolyte that can circumvent study by DLS.

This idea was proposed by Russo et al. and a study of 100% sulfonated NaPSS and fluorescently labeled NaPSS was performed.⁴⁶ The problem with this study was the collection of low PDI samples: GPC was used to fractionate the polymer, making the yield very low. This is solved by using a controlled synthesis of NaPSS. Large amounts of sample can be prepared via a living polymerization, providing a narrow PDI.

Chapter 4 Fluorescence Photobleaching Recovery

4.1 Fluorescent Studies of Polyelectrolytes

FPR is used when the sample is fluorescent, or if it can be labeled with a fluorescent dye. Many different dyes can be attached but FPR is not always the best technique for finding the diffusion coefficient.⁴⁹ Analytical Ultracentrifugation, AUC, has been used to probe the slow mode diffusion,⁸ but AUC is better suited for experiments using a small amount of sample.¹ Pulsed Field gradient NMR spectroscopy (DOSY) can be used for very fast diffusers and DLS can find diffusion coefficients.^{1,50} FPR is well suited for this work because dust does not need to be excluded as in DLS, it can probe longer distance scales than DLS, and polystyrene sulfonate is not a very fast diffuser (although FPR can find fast diffusers as well).

There have been several studies performed with fluorescent polyelectrolytes and even fluorescent polystyrene sulfonate.^{10,46,51-53} The diffusion coefficient found for fluorescent polystyrene sulfonate with FPR was in-between the fast and slow modes found in DLS, but was not the average of them. The conclusion was the slow mode was caused by aggregates that existed on a time scale shorter than FPR probes. The problem with this study was the PSS labeled had the possibility of hydrophobic patches along the backbone.⁴⁶ Another study investigated the diffusion of fluorescently labeled polystyrene in semidilute and concentrated polymer solutions.⁵⁴ This is different than the present study because polystyrene sulfonate was not used but they found the diffusion coefficient decreased upon increasing polymer concentrations. They also used fluorescence correlation spectroscopy (FCS). For a FCS experiment, the changes in fluorescence are followed and the fluctuations are fit to a correlation function. This experiment functions very similar to DLS and so probes the same distance scales.

4.2 Experimental Background

The experimental background has been adapted from a chapter 10 from *Soft Matter: Scattering Imaging and Manipulation*.¹ In a fluorescence photobleaching recovery experiment a laser illuminates the

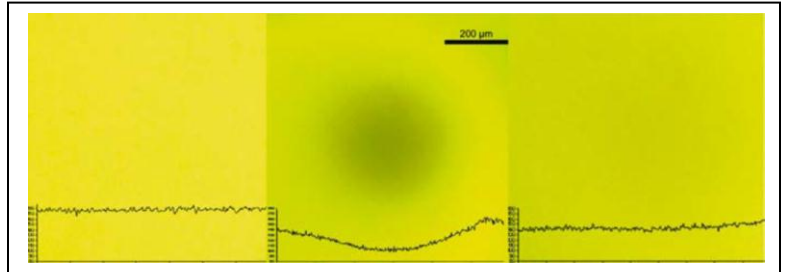


Figure 4.1 The left image shows the background fluorescence. The middle image shows a dark spot that is due to bleaching. The right shows the return of the fluorescence. Taken from Reference 1. Reprint with permission from Springer.

sample and the background fluorescence is measured. A brief, intense pulse bleaches the sample and the return of the fluorescence is measured.^{55,56} Figure 4.1 shows the baseline fluorescence, bleaching (the dark spot and decrease in fluorescence intensity), and the return of the fluorescence. Different types bleaching can be performed (see Figure 4.2). For a spot bleaching, the fluorescent intensity, $F_k(t)$, is found by

$$\frac{F(0)}{F^0} = \frac{(1-e^{-k})}{k} \quad \text{Equation 4.1}$$

where k is the depth parameter, F^0 is the pre-bleach intensity, and $F(0)$ is the immediate post-bleach intensity.¹ To find the percent of dye molecules bleached

$$P = \frac{F^0 - F(0)}{F^0} \times 100 \quad \text{Equation 4.2}$$

To find the diffusion coefficient the intensity is fit to Equation 4.3.

$$f(t) = e^{(-2\tau_D/t)} \left[I_0 \left(2\tau_D/t \right) + I_1 \left(2\tau_D/t \right) \right] \quad \text{Equation 4.3}$$

I_0 and I_1 are Bessel functions and

$$\tau_D = \frac{w^2}{4D} \quad \text{Equation 4.4}$$





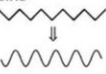

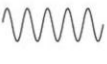
Category	Pattern	Detected	Ref.	Comments
Spot	 Gaussian spot	Profile itself	2,3	Most common.
Spot	 Square spot	Profile itself	44	
Stripe	 Ronchi ruling $K = 2\pi/L$	Sum of Fourier components of square wave	5,6	Provides periodic boundary condition.
Modulated	 Ronchi ruling	Usually triangle wave filtered to sine 	47	Enables shallow bleaches, each diffuser produces a single exponential decay.
	 Crossed beams	Depends on modulation scheme 	16,54,55	Enables much shorter spatial distances.
Video	Varies Mask	FFT	112	Fewer moving parts, multiple K values simultaneously measured.

Figure 4.2 Various types of bleaching patterns. Taken from reference 1. Reprint with permission from Springer.

where w is the half-width of the beam and D is the diffusion coefficient. FPR can yield diffusion coefficients in a wide range: 1×10^{-5} to $< 10^{-14} \text{ cm}^2 \text{ s}^{-1}$.¹

Along with a wide range for the diffusion coefficient, many different types of samples can be used.^{57,58} When attaching the dye, a beginning is to use enough dye to label one in every ten to one hundred repeat units. It is also important to choose a dye that has an

absorption maximum in the proper wavelength (needs to match the laser output).

A potential source of error for FPR is unreacted dye present in the sample. Purification techniques such as precipitation or dialysis sometimes need be performed to eliminate free dye. The free dye can be ignored by fitting a 2 EXP or eliminating a few channels of the recovery trace. Along with attaching the dye, it is important the polymer structure does not change after labeling.¹ It is assumed in an FPR experiment that the fluorescent dye does not change the structure of the analyte. Investigation using gel permeation chromatography with light scattering, DLS, DOSY, and phase behavior show if the polymer was affected. It is also assumed that after the bleach pulse the difference in structure between the non-bleached and bleached molecules is small; thus, the chemical potential difference and thermodynamic driving force $d\mu/dc$ are small. This means FPR is an experiment almost independent of thermodynamic interactions that dictate

the DLS experiment. Yu et al.. have also shown that the location of the labeling, whether it is in the middle of the chain or the end group, is inconsequential for the studied polymer.⁵⁹

A representative FPR experimental setup is found in figure 4.3. A Ronchi ruling is used in our experimental set up because of its easy availability and production a square wave of intensity on the sample. A Ronchi ruling is glass slide that has black lines at regular intervals, where the spatial frequency is $k = 2\pi/L$ and L is the spacing between lines.¹ For a stripe pattern bleaching the intensity is as follows,

$$F(x, t = 0) = F^0 - \frac{C}{2} + \frac{C}{2} \left[\frac{4}{\pi} \left((\sin(Kx) + \frac{1}{3}\sin(3Kx) + \frac{1}{5}\sin(5Kx) + \frac{1}{7}\sin(7Kx) + \dots) \right) \right]$$

Equation 4.5

$$C = |F^0 - F_{min}(t = 0)| \quad \text{Equation 4.6}$$

C is the initial contrast, where $F_{min}(t = 0)$ is the minimum intensity along the square wave. Equation 4.5 is the Fourier series for the square wave of intensity, having fundamental and odd harmonics. Each harmonic relaxes as a multiple of the fundamental harmonic, $e^{(-DK^2t)}$. For example, the third harmonic decays 9 times faster and the fifth decays 25 times faster. The higher harmonics present are due to “multiple, simultaneous instances of diffusion in a sine wave boundary condition.”¹ Because the higher harmonics disappear so quickly, they can be ignored and the fluorescence can be described as

$$F(t) = F^0 - \frac{C}{2} - \frac{C}{2} \left(\frac{e^{(-DK^2t)} + \frac{1}{3}e^{(-9DK^2t)} + \dots}{1 + \frac{1}{3} + \dots} \right) \quad \text{Equation 4.7}$$

In this lab, the striped pattern is modulated by moving the Ronchi ruling back and forth.⁶⁰ Equation 4.5 shows multiple exponential terms are associated with one diffuser. This becomes much more complicated when multiple diffusers are present, e.g. polydisperse samples. The movement of the Ronchi ruling and a tuned in amplifier select only the fundamental frequency.

Using the Ronchi ruling creates a triangle wave by moving the Ronchi ruling perpendicularly to the stripes being bleached. The triangle wave has a frequency ω , dependent upon the speed at which the Ronchi ruling is moved and its spacing.¹ The new triangle wave can be described by

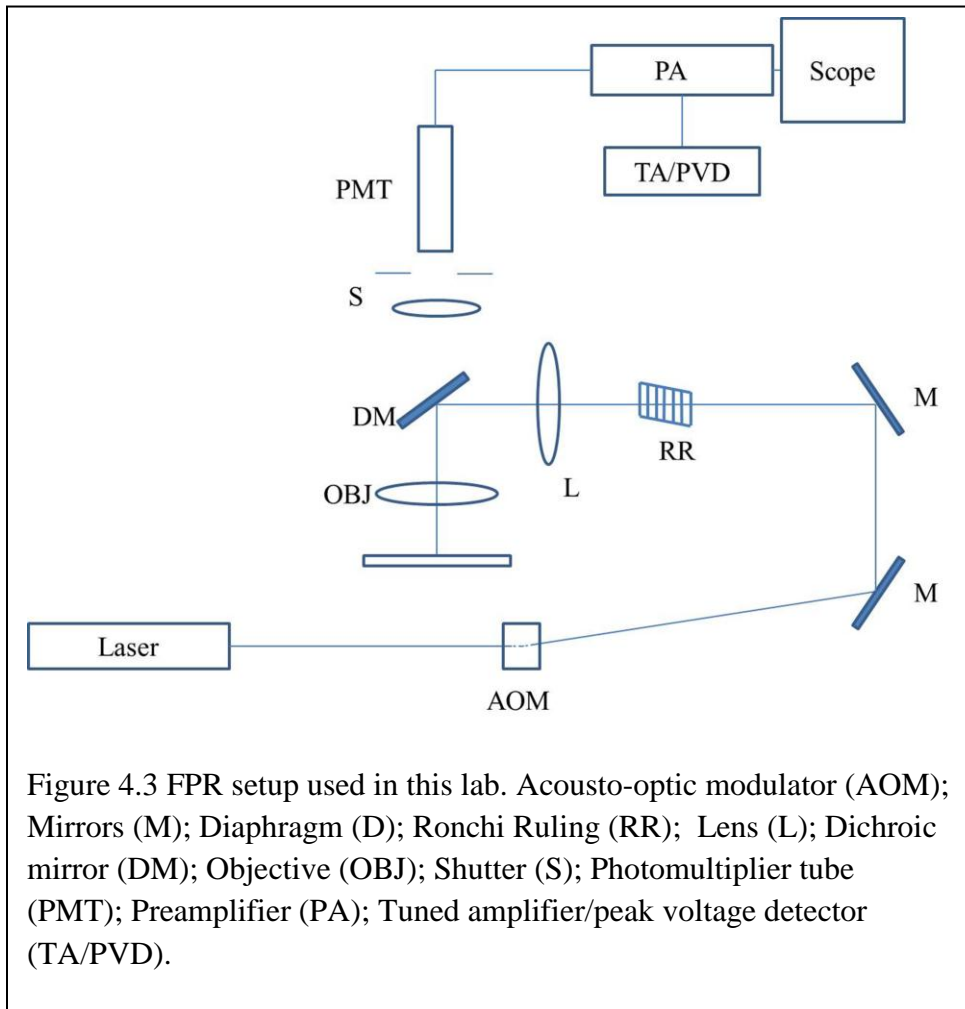
$$V(t) \propto C_1(t) \sin(\omega t) - C_3(t) \sin(3\omega t) - C_5(t) \sin(5\omega t) - \dots$$

Equation 4.8

where the contrast decay is

$$C_n(t) \propto \frac{1}{n^2} e^{-n^2 K^2 D t} \quad \text{Equation 4.9}$$

The higher harmonics will decrease more rapidly than before due to the n^2 term in the



denominator for Equation 4.9. This would be a bad thing except the fundamental frequency can be found with the aid of a lock-in amplifier.^{1, 60, 61} Thus, very shallow bleaches can be performed and only a single exponential decay is found.

Chapter 5 Polystyrene Sulfonate

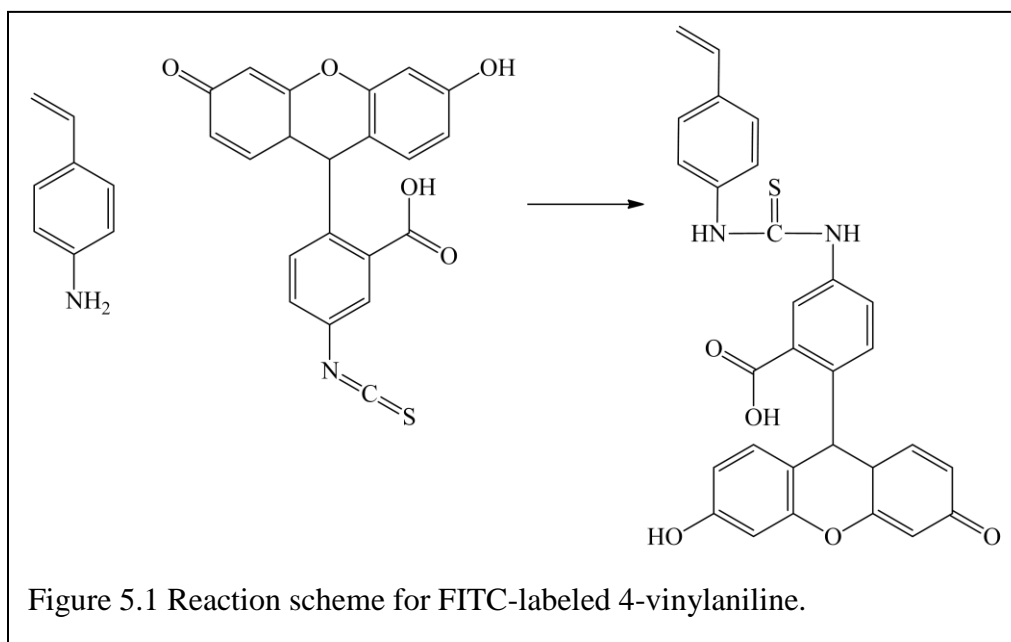
5.1 Experimental

5.1.1 Materials

4-styrene sulfonic acid sodium salt hydrate (CAS: 123333-94-8), bromo-p-toluic acid (97%), and fluorescein isomer 1 (FITC) were purchased from Sigma Aldrich. Copper (I) chloride (99.9995+%), 2-2'-bipyridine (99+%), and vinyl aniline (90%) were purchased from Acros. Methanol was purchased from Fisher Scientific. All chemicals purchased were used with no further purification. The water used was purified by a Barnstead Nanopure water system.

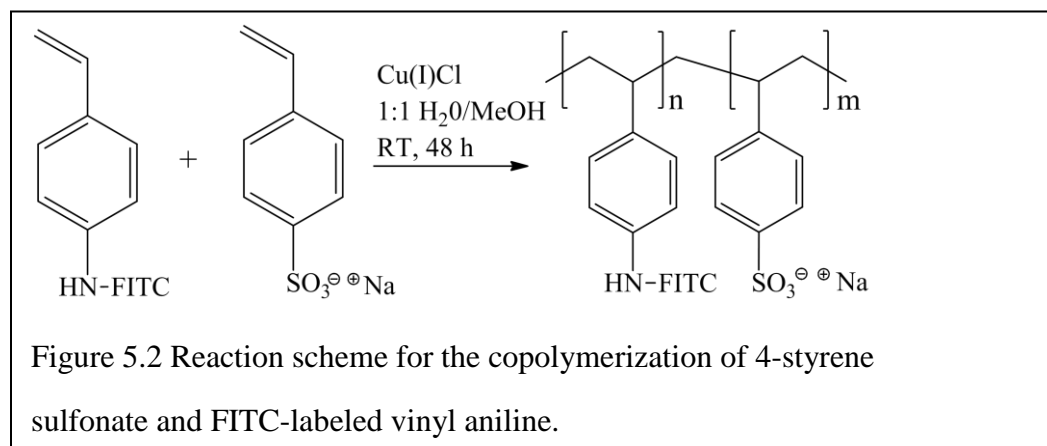
5.1.2 Synthesis of FITC-labeled Vinylaniline

38 mg (0.09 mmol) of FITC isomer 1 was dissolved in 8 mL 200-proof ethanol in a round-bottom flask. The flask was purged with N₂ and then 10 μ L of vinylaniline were added via syringe. The reaction was heated to 50° C for 1 hour and stirred at room temperature for 24 hours. The solvent was evaporated and the solid was stored. Some degradation was noted if the solution was heated during solvent evaporation.



5.1.3 Synthesis of FITC-labeled Polystyrene Sulfonate Sodium Salt

4.89 g (21.3 mmol) of 4-styrene sulfonic acid sodium salt hydrate was dissolved in 22 mL water (purged with N₂ for 30 min) in a round-bottom flask. Once the 4-styrene sulfonic acid sodium salt hydrate was dissolved 51 mg (0.24 mmol) of bromo-p-toluic acid was added and 1M NaOH was added drop-wise until the pH was ~ 10. The FITC-labeled vinylaniline was dissolved in 6 mL methanol (purged with N₂ for 30 min) and added to the reaction vessel after the pH was ~ 10. The reaction vessel was degassed with N₂ for 30 minutes followed by adding 24 mg (0.24 mmol) Cu(I)Cl and 74 mg (0.48 mmol) 2-2'-bipyridine in a customized glove box. The reaction was allowed to proceed for 48 hours before being terminated by opening to the atmosphere and adding 5 mL water and 5 mL methanol. The reaction mixture was then purified by a silica column. Flash chromatography could not be used because the copper would elute with the polymer. The reaction mixture was precipitated in 450 mL acetone three times, dried, and dissolved in a dialysis bag with a molecular weight cutoff of 6-8,000 g/mol (~45 mL). During the first day the dialysis water was changed every 2 hours. Subsequently, for the next three days the dialysis water was changed twice daily. The dialysis was continued until no fluorescence was seen in the dialysis water upon illumination with blue laser light. It is important not to heat the polymer during drying because some degradation was noted.



5.1.4 Synthesis of Polystyrene Sulfonate

The procedure is identical to the FITC-labeled NaPSS without the addition of the fluorescent monomer. Specifically, 4.89 g (21.3 mmol) of 4-styrene sulfonic acid sodium salt hydrate was dissolved in 22 mL degassed (purged with N₂ for 30 min) water and 22 mL methanol in a round-bottom flask. Once the 4-styrene sulfonic acid sodium salt hydrate was dissolved 51 mg (0.24 mmol) of bromo-*p*-toluic acid was added and 1M NaOH was added dropwise until the pH was ~ 10. The reaction vessel was degassed with N₂ for 30 minutes followed by adding 24 mg (0.24 mmol) Cu(I)Cl and 74 mg (0.48 mmol) 2-2'-bipyridine. The reaction was allowed to proceed for 48 hours before being terminated by opening to the atmosphere and adding 5 mL water and 5 mL methanol. The reaction mixture was then purified by a silica column. Flash chromatography could not be used because the copper would elute with the polymer.

5.2 Characterization

- **Molecular Weight Distribution.** The molecular weight and polydispersity index were obtained using GPC/MALLS using a Wyatt DAWN DSP-F with a Helium-Neon laser. Two ISCO 500 mL pumps were used to prevent pulsing during pumping, the sample was injected manually, and the columns were PL Aquagel-OH Mixed 8 μm (2x) protected by a PL Aquagel 8 μm guard column. A Waters 410 differential refractive index detector was used and the samples were analyzed with ASTRA V 4.7. The specific refractive index increment, dn/dc , was taken as 0.198 mL/mg.⁶² Samples were dissolved in the mobile phase, 200 mM NaNO₃ + 10 mM NaH₂PO₄ + 2 mM NaN₃ adjusted to pH 7.5. The injected volume was 100 μL and the flow rate was 0.5 mL/min. The weight-average molecular weight and its standard deviation were calculated from three or more repeat measurements.

- **^1H NMR Spectra.** ^1H NMR spectra were acquired on a Bruker APX 250 MHz spectrometer at 25 °C. The product was dissolved in D_2O .

- **Fluorescence Spectroscopy.**

Fluorescence studies were carried out with a PTI QuantaMaster4/2006SE spectrofluorimeter.

5.3 Results and Discussion

5.3.1. FITC-Labeled Vinyl Aniline

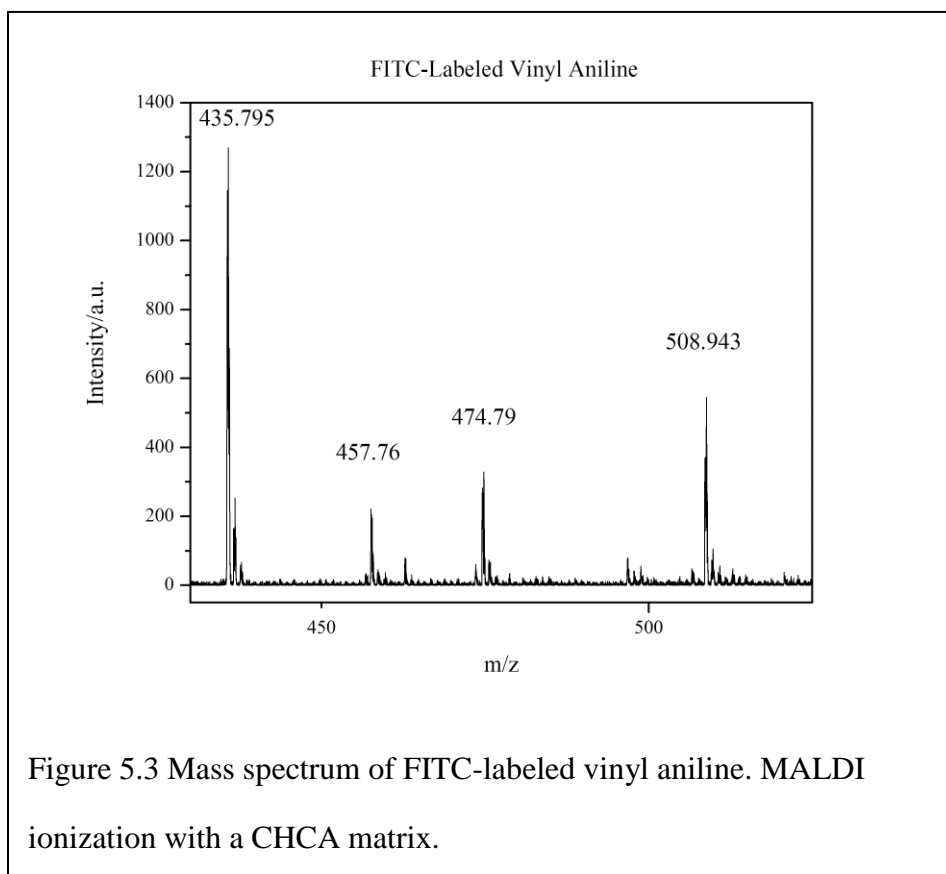


Figure 5.3 is a MALDI spectrum with a α -cyano-4-hydroxycinnamic acid (CHCA) matrix of FITC-labeled vinyl aniline. The peak at 508.943 m/z corresponds to the molecular ion. The other peaks, 474.79 m/z, and 457.76 m/z are unexplained. They are not due to free FITC and do not correspond to fragments from the product. The peak at 435.795 m/z is consistent with a

side reaction, ethanol adding to FITC instead of the vinyl aniline. If this is true, there exists the possibility that some unreacted vinyl aniline was incorporated into the NaPSS copolymer. A usual loading is ~1 % so any unreacted vinyl aniline should have little to no effect, and much less than having ~10 % non-sulfonated side chains as in a typical NaPSS synthesis.

The synthesis was variable, meaning that two different batches had the molecular ion peak present, but the secondary peaks will change. For example, one batch that was characterized using ESI ionization in place of MALDI had fragments of the product (as expected). Other batches, only investigated with MALDI, showed different peaks and have little to no fragments from the product. The variability is discussed in section 5.3.4.

5.3.2 Unlabeled Polystyrene Sulfonate

As previously stated, the fluorescent and unlabeled NaPSS were synthesized in similar fashions. It was believed that the fluorescent NaPSS should behave similarly to the unlabeled or “patchless” NaPSS during polymerization. Table 5.1 shows characterization data for three samples of NaPSS.

Table 5.1 Molecular Weight Characterization of NaPSS

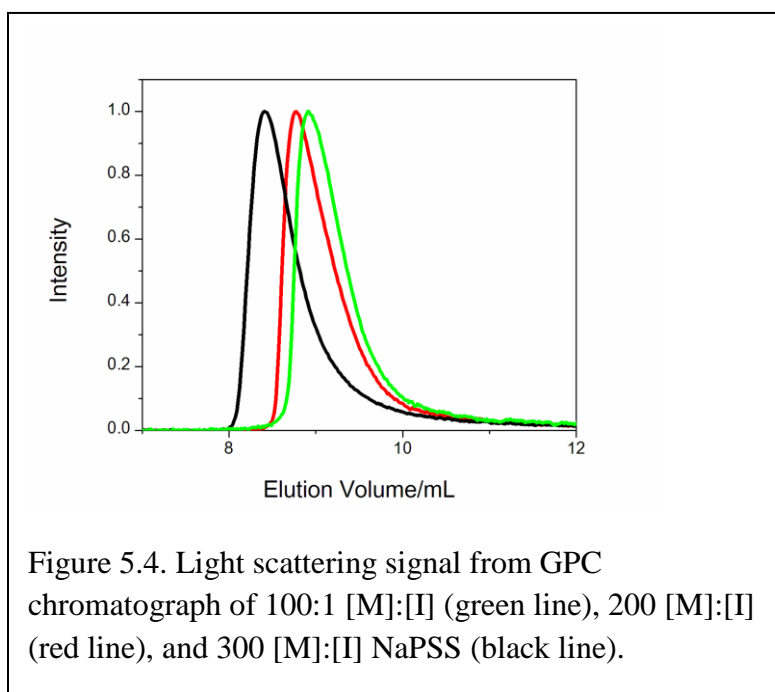
Sample #	Sample	[M]/[I]	Theoretical M_n	M_n	M_w	PDI
WH.2.47	NaPSS	100:1	18,300	61,300±500	67,000±600	1.10±0.1
WH.2.48	NaPSS	200:1	40,400	67,000±1,500	82,400±1,400	1.23±0.1
WH.2.50	NaPSS	300:1	55,300	175,200±5,400	194,900±4,300	1.11±0.1

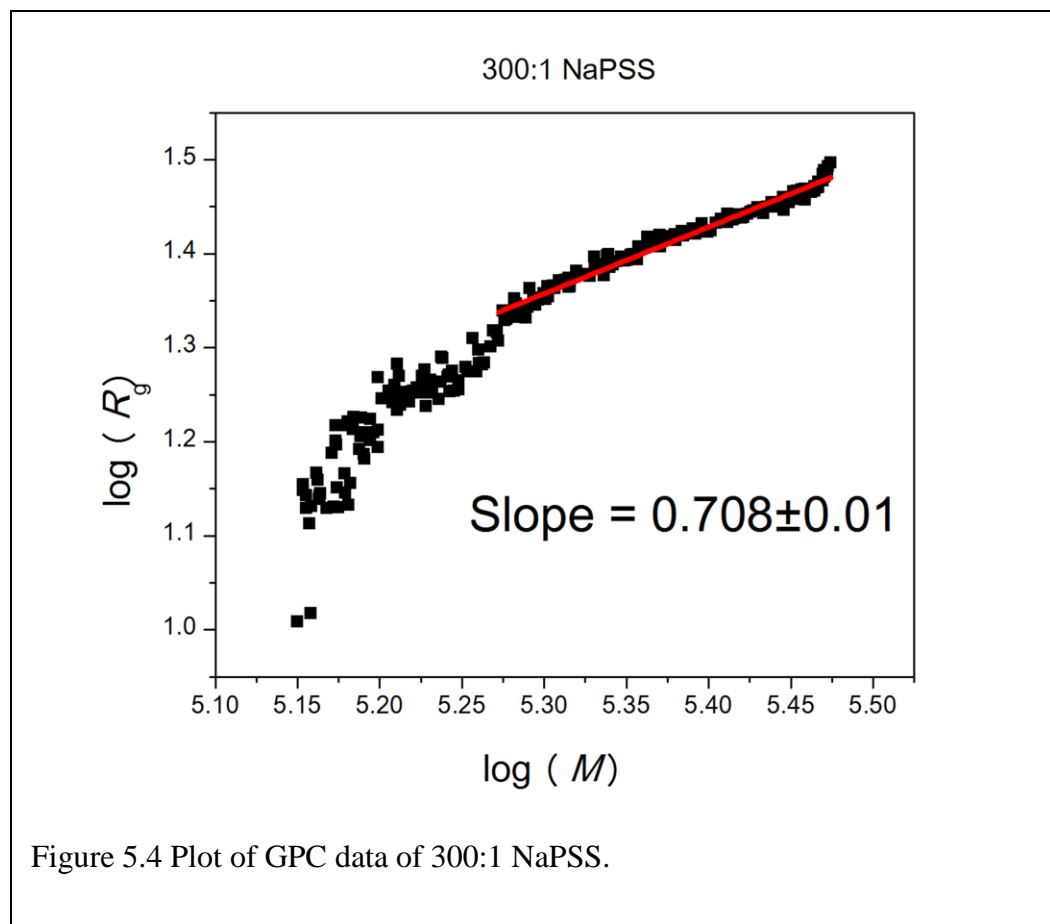
Molecular weights were calculated from GPC/MALLS. $dn/dc = 0.198 \text{ mL/g}$.

The molecular weight increased with increasing monomer:initiator ratio ([M]:[I]), but not in a predictable way. There was little difference between the 100:1 [M]:[I] and 200 [M]:[I]

loadings, but a large difference with 300 [M]:[I]. The PDI was low, and does not change much as the [M]:[I] loading was increased. The syntheses for the unlabeled NaPSS showed an inconsistent increase in molecular weight. A GPC trace is found in Figure 5.4. The peaks are unimodal and the elution time decreases as the molecular weight increases. There appears to be a tail to the peak, indicating many smaller polymers present.

From the GPC trace a plot of $\log(R_g)$ vs. $\log(M)$ a linear fit to a portion of the data shows a slope of 0.708 ± 0.010 (Figure 5.4). The lower values of R_g were not included in the fit because there is more noise at the low size. The fit starts at the point where the data start to become linear and less noisy. A 300:1 [M]:[I] sample was chosen because it had the largest radius. The lower initiator loadings resulted in data that was too noisy to add a fit. The slope of 0.708 ± 0.010 shows the polymer is not a random coil (slope = 0.5 – 0.6), and is starting to become more rigid (slope of rod = 1). The polymer was not expected to be a rigid rod because the GPC solvent was not low salt





5.3.3 Fluorescent Polystyrene Sulfonate

FITC-NaPSS was synthesized in a similar way to the unlabeled NaPSS, but with addition of FITC-labeled vinyl aniline. A comparison of two trials is found in table 5.2. Mirroring the problem in the patchless NaPSS, the molecular weights do not increase predictably with increasing [M]:[I]. To further complicate the problem, with the same [M]:[I] loadings do not give the same molecular weight. The PDI begins low and creeps up as the [M]:[I] loading increases. A GPC trace can be found in Figure 5.5. The GPC traces are unimodal and have a tail just like the unlabeled NaPSS but it is less pronounced. This is likely due to the more vigorous work-up.

A plot of $\log(R_g)$ vs. $\log(M)$ for the 300:1 [M]:[I] loading shows the slope was 0.652 ± 0.003 . Once again, the lower radii were not included in the fit because they exceed the

sensitivity of our instrument. A sample of 300:1 [M]:[I] was chosen because lower initiator loadings resulted in data with too much noise for reliable data fitting. A slope of 0.652 ± 0.003 is smaller than the corresponding patchless NaPSS but this may be attributed to variability in the samples. The FITC-NaPSS polymer was not a rigid rod but was stiffer than a random coil.

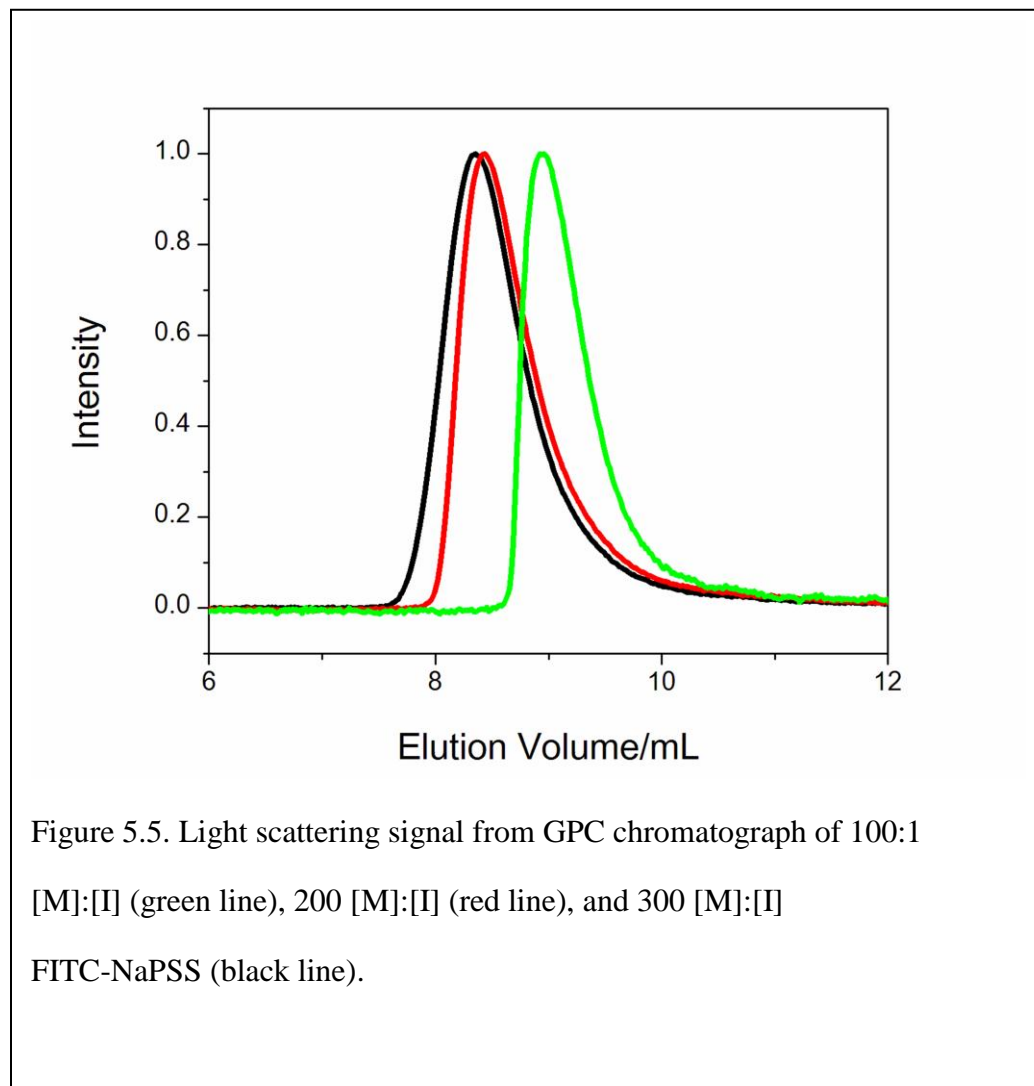
Table 5.2 Molecular Weight Characterization of FITC-NaPSS

Sample	[M]/[I]	Theoretical M_n	M_n	M_w	PDI
Trial 1					
FITC-NaPSS	100:1	18,100	$55,000 \pm 680$	$58,400 \pm 6,600$	1.06 ± 0.01
FITC-NaPSS	200:1	41,000	$148,000 \pm 3,200$	$173,900 \pm 3,100$	1.17 ± 0.01
FITC-NaPSS	300:1	56,100	$168,700 \pm 6,200$	$209,500 \pm 4,500$	1.24 ± 0.01
Trial 2					
FITC-NaPSS	100:1	18,100	$38,100 \pm 160$	$40,100 \pm 380$	1.06 ± 0.01
FITC-NaPSS	200:1	41,000	$60,800 \pm 900$	$66,300 \pm 520$	1.08 ± 0.01
FITC-NaPSS	300:1	56,100	$68,000 \pm 1,300$	$88,900 \pm 1,400$	1.30 ± 0.01

Molecular weights and PDI were found using GPC/MALLS.

The polymerization of NaPSS has been shown to be a living polymerization for up to 8 hours and was the basis for the current synthesis.⁶³ The current polymerization was allowed to react for 48 hours so it was believed that side reactions were prevalent at such long reaction times. Therefore, a time-dependent study of molecular weight was performed (Table 5.3). Along with monitoring the molecular weights as a function of time, the solid catalyst was now added in a custom glove box. This should minimize the possibility for oxygen to enter the reaction vessel.

The aliquots were each taken in the glove box as well to eliminate excess oxygen. It can be seen than the molecular weight inconsistently oscillates. Also, the molecular weights are much lower than previous samples. It is unknown why the molecular does not solely increase with time.



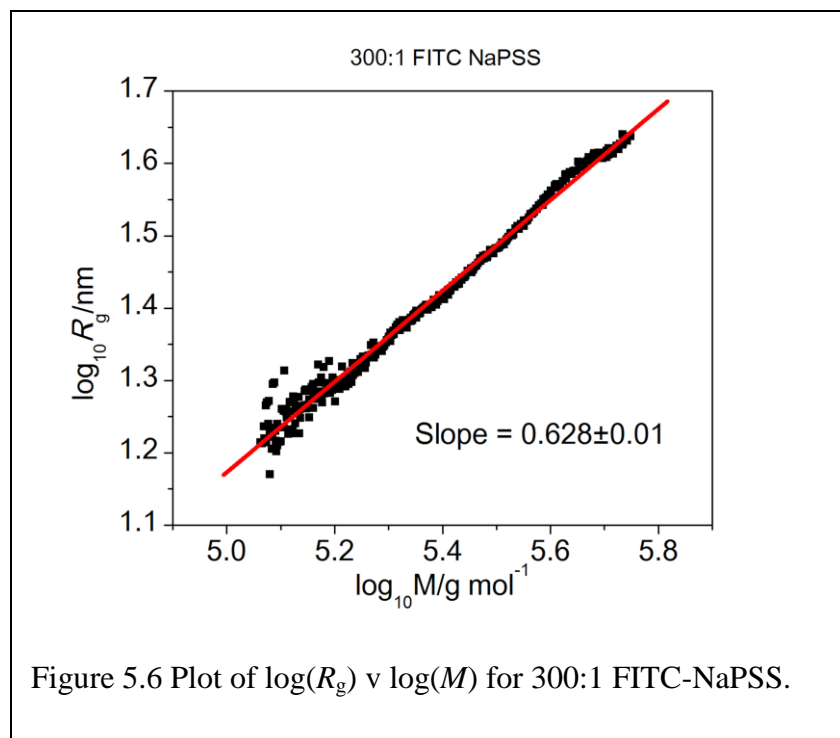
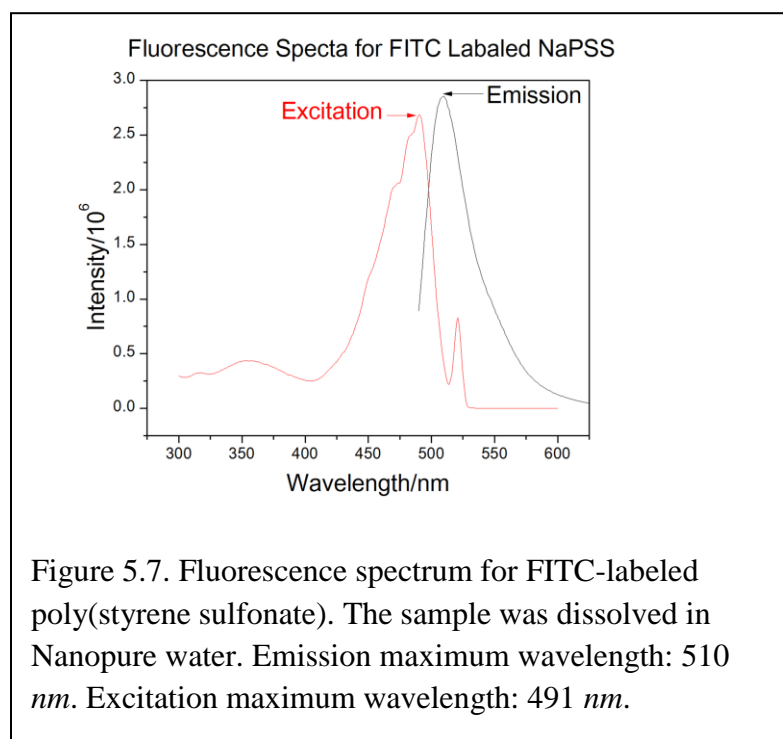


Table 5.3 Molecular Weight Characterization of FITC-NaPSS as a Function of Time

1% FITC Loading				2% FITC Loading		
Hour	M_n	M_w	PDI	M_n	M_w	PDI
1	23,900±100	25,000±210	1.05±0.01	26,000 ±400	27,300±940	1.05±0.02
2	14,000±250	15,700±700	1.13±0.03	30,200 ±170	31,500±90	1.04±0.01
3	14,400±250	17,200±780	1.20±0.03	24,600±140	26,000±180	1.05±0.01
4	28,700±70	32,000±360	1.13±0.03	27,000 ±220	28,700±800	1.06±0.02
6	-	-	-	21,400±90	24,600±1,400	1.15±0.05
24	15,100±420	17,400±680	1.15±0.04	21,000 ±250	22,370 ±760	1.06±0.02
48	16,400±230	19,100±650	1.17±0.03	15,500±250	16,200±620	1.06±0.02

Molecular weight and PDI were found using GPC/MALLS. Both 1 % and 2 % used a 100:1 [M]:[I] loading.

The presence of fluorescence in the FITC NaPSS was confirmed by spectrofluorimetry. The maximum absorbance was 489 nm and the emission was 510 nm (Figure 5.7).

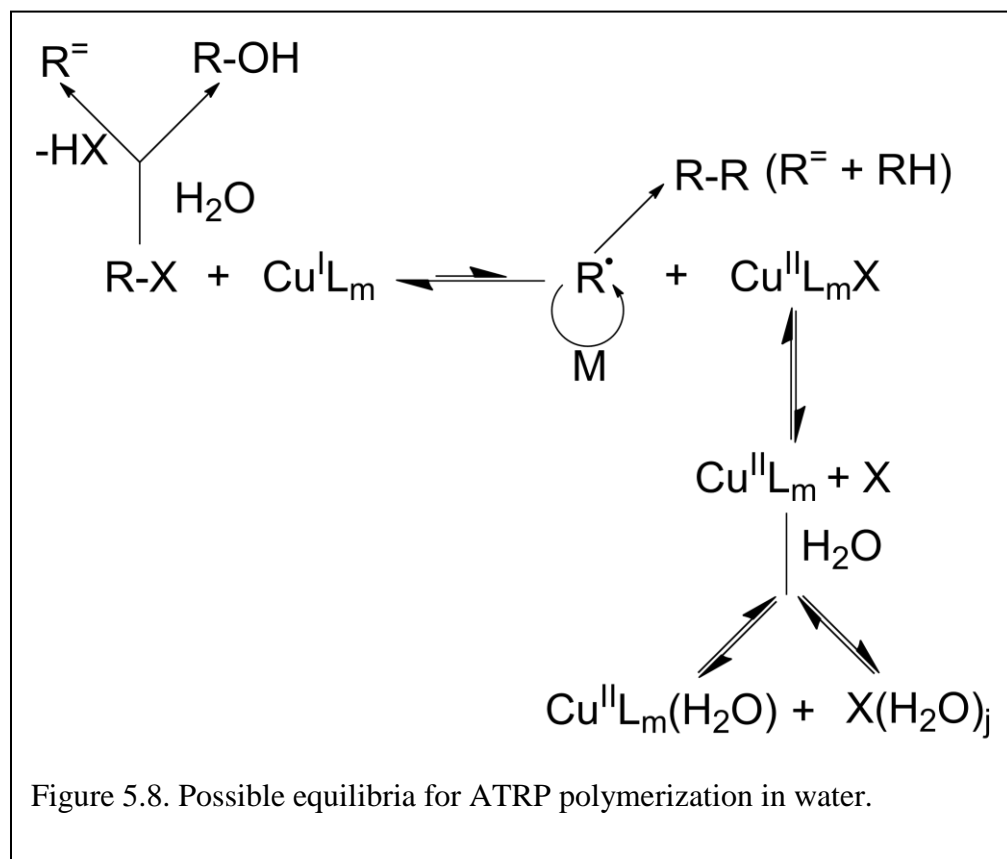


5.3.4 Possible Causes of Unpredictable Molecular Weight

Several possibilities exist for the molecular weight being inconsistent. First, FITC may produce radicals.⁶⁴ This could cause side reactions during the polymerization, decreasing the molecular weight. Also, molecular oxygen may be present in the reaction, thus affecting the molecular weight. Oxygen is prohibited because it can react with the radical and increase the molecular weight. Further, because ATRP is a living polymerization, a reversible addition of the halogen will end-cap the polymer chain. It was noted that partial hydrolysis of the halogen-capped polymer chain can cause loss of control over the molecular weights.^{63,65}

Although the previous reasons will affect the molecular weight, the more likely reason is the problem of ATRP synthesis in protic solvents, and especially water.⁶⁵ Many equilibria are

happening and may cause inconsistent molecular weights. Also, the synthesis is expected to be very quick due to the addition of water to $\text{Cu}^{\text{II}}\text{L}_m\text{M}$ and a large PDI is expected. In our synthesis the reaction happens quickly (Table 5.3) and is much higher than expected molecular weight, but the PDI is low. Therefore, it is believed the most likely cause of variable molecular weights is the difficulty in adding the catalyst. In our synthesis the solid catalyst is weighed and added to the reaction flask. Therefore, some of the catalyst may stick on the neck of the flask, etc.



Using a solution of the catalyst and ligand would be ideal, but requires a large volume of solvent to dissolve a small amount of catalyst and ligand. Different ligands, specifically water soluble ligands, may be tried. Another method to help control the molecular weight is using argon in place of nitrogen and purging the solvents for longer than 30 minutes. It was found that purging

with nitrogen removed oxygen but it is reversible.⁶⁶ With argon being heavier than air, it should be a slower reversibility and prevent oxygen during the reaction.

5.4 Conclusions

The synthesis of a fluorescent and unlabeled polystyrene sulfonate herein does not provide a living polymerization. Different molecular weights can be synthesized, therefore, a wide range of molecular weights are available for study. No claim is made regarding the control of synthesis; while it is an intriguing synthetic problem, the method developed does produce large amounts of low-polydispersity polymers for physical investigations. While it is disappointing that currently the molecular weight is not controllable, it is still under investigation; however, the usefulness of this polymer lies not in its synthesis but its use. In order to study the slow mode decay a polymer that is absent of any hydrophobic defects should be used; therefore, in this research, a fluorescent NaPSS has been synthesized that is patchless and can be used to study the slow mode decay in conjunction with FPR. FPR is suited for studying the slow mode decay because it is independent of thermodynamic interactions like DLS, it has an easier sample preparation than DLS, it can measure the same and larger distance scales than DLS, and the experiment is shorter than DLS. Because of this, it is believed FPR offer new insights into one of the most challenging of polymer topics, the cause of the slow mode decay.

References

1. Russo, P. Q., J.; Edwin, N.; Choi, Y.W.; Doucet, G. J.; Sohn, D., Fluorescence Photobleaching Recovery. In *Soft Matter: Scattering Imaging and Manipulation*, 2008.
2. Lin, S. C.; Lee, W. I.; Schurr, J. M. *Biopolymers* **1978**, 17, (4), 1041-1064.
3. Lichter, J. A.; Van Vliet, K. J.; Rubner, M. F. *Macromolecules* **2009**, 42, (22), 8573-8586.
4. M.Yang, X.-C.; Samanta, B.; Agasti, S. S.; Jeong, Y.; Zhu, Z.-J.; Rana, S.; Miranda, O. R.; Rotello, V. *Angewandte Chemie International Edition* **2011**, 50, (2), 477-481.
5. Zheludkevich, M. L.; Shchukin, D. G.; Yasakau, K. A.; Möhwald, H.; Ferreira, M. G. S. *Chemistry of Materials* **2007**, 19, (3), 402-411.
6. Xu, Y.; Mazzawi, M.; Chen, K.; Sun, L.; Dubin, P. L. *Biomacromolecules* **2011**, 1512-1522.
7. Lee, S. W.; Lee, H. J.; Choi, J. H.; Koh, W. G.; Myoung, J. M.; Hur, J. H.; Park, J. J.; Cho, J. H.; Jeong, U. *Nano Letters* **2009**, 10, (1), 347-351.
8. Luo, Z. L.; Zhang, G. Z. *Macromolecules* **2010**, 43, (23), 10038-10044.
9. Lodge, T.; Hiemenz, P., *Polymer Chemistry*. Second ed.; CRC Press: Boca Raton, 2007.
10. Sohn, D.; Russo, P. S.; Dávila, A.; Poche, D. S.; McLaughlin, M. L. *Journal of Colloid and Interface Science* **1996**, 177, (1), 31-44.
11. Gabriel, D. J., Charles, *Laser Light Scattering*. General Publishing Company: Toronto, 1981; p 96.
12. Russo, P. Virtual Macro Book.
<http://macro.lsu.edu/CoreCourses/MSweb4/VirtualMacroBook.htm> (5-4).
13. Harwood, W. H., Geoffrey; Petrucci, Ralph., *General Chemistry Principles and Modern Applications*. 8 ed.; Prentice-Hall, Inc.: Upper Saddle River, 2002.
14. Russo, P. S.; Fong, B.; Temyanko, E.; Ricks, H.; Poche, D. S. *Journal of Chemical Education* **1999**, 76, (11), 1534.
15. Kreuer, K. D. *Journal of Membrane Science* **2001**, 185, (1), 29-39.
16. Liger-Belair, G.; Prost, E.; Parmentier, M.; Jeandet, P.; Nuzillard, J.-M. *Journal of Agricultural and Food Chemistry* **2003**, 51, (26), 7560-7563.
17. Lee, W. I.; Schurr, J. M. *Journal of Polymer Science Part B-Polymer Physics* **1975**, 13, (5), 873-888.

18. Sedlak, M.; Amis, E. J. *The Journal of Chemical Physics* **1992**, 96, (1), 817-825.
19. Goinga, H. T.; Pecora, R. *Macromolecules* **1991**, 24, (23), 6128-6138.
20. Forster, S.; Schmidt, M.; Antonietti, M. *Polymer* **1990**, 31, (5), 781-792.
21. Mathiez, P.; Mouttet, C.; Weisbuch, G. *Biopolymers* **1981**, 20, (11), 2381-2394.
22. Sedlak, M.; Konak, C.; Stepanek, P.; Jakes, J. *Polymer* **1987**, 28, (6), 873-880.
23. Zhou, K. J.; Li, J. F.; Lu, Y. J.; Zhang, G. Z.; Xie, Z. W.; Wu, C. *Macromolecules* **2009**, 42, (18), 7146-7154.
24. Sedlak, M. *Journal of Chemical Physics* **1996**, 105, (22), 10123-10133.
25. Fuoss, R. M.; Katchalsky, A.; Lifson, S. *Proceedings of the National Academy of Sciences of the United States of America* **1951**, 37, (9), 579-589.
26. Lifson, S.; Katchalsky, A. *Journal of Polymer Science* **1954**, 13, (68), 43-55.
27. Degennes, P. G.; Pincus, P.; Velasco, R. M.; Brochard, F. *Journal De Physique* **1976**, 37, (12), 1461-1473.
28. Daoud, M.; Cotton, J. P.; Farnoux, B.; Jannink, G.; Sarma, G.; Benoit, H.; Duplessix, C.; Picot, C.; de Gennes, P. G. *Macromolecules* **1975**, 8, (6), 804-818.
29. Kosmas, M. K.; Freed, K. F. *Journal of Chemical Physics* **1978**, 69, (8), 3647-3659.
30. Odijk, T. *Macromolecules* **1979**, 12, (4), 688-693.
31. Tong, X. A Novel Synthesis and Characterization of Fluorescein Isothiocyanate Labeled Poly(styrene sulfonate sodium salt). Louisiana State University, Baton Rouge, 2009.
32. Drifford, M.; Dalbiez, J. P. *The Journal of Physical Chemistry* **1984**, 88, (22), 5368-5375.
33. Katchalsky, A. *Pure Appl. Chem.* **1971**, 26, (3-4), 327-374.
34. Schurr, J. M.; Schmitz, K. S. *Annual Review of Physical Chemistry* **1986**, 37, 271-305.
35. Bruno, K. R.; Mattice, W. L. *Macromolecules* **1992**, 25, (1), 327-330.
36. Stigter, D. *Biopolymers* **1979**, 18, (12), 3125-3127.
37. Schmitz, K. S. *Accounts of Chemical Research* **1996**, 29, (1), 7-11.

38. Drifford, M.; Dalbiez, J. P. *Biopolymers* **1985**, 24, (8), 1501-1514.
39. Ermi, B. D.; Amis, E. J. *Macromolecules* **1998**, 31, (21), 7378-7384.
40. Muthukumar, M. *Journal of Chemical Physics* **1996**, 105, (12), 5183-5199.
41. Ray, J.; Manning, G. S. *Langmuir* **1994**, 10, (7), 2450-2461.
42. Schmitz, K. S. *Langmuir* **1997**, 13, (22), 5849-5863.
43. Forster, S.; Schmidt, M., Polyelectrolytes in Solution. In *Physical Properties of Polymers*, Springer-Verlag Berlin: Berlin 33, 1995; Vol. 120, pp 51-133.
44. GronbechJensen, N.; Mashl, R. J.; Bruinsma, R. F.; Gelbart, W. M. *Physical Review Letters* **1997**, 78, (12), 2477-2480.
45. Budd, P. *Prog. Colloid Polym. Sci.* **1994**, 94, 107-115.
46. Cong, R. J.; Temyanko, E.; Russo, P. S.; Edwin, N.; Uppu, R. M. *Macromolecules* **2006**, 39, (2), 731-739.
47. Topp, A.; Belkoura, L.; Woermann, D. *Macromolecules* **1996**, 29, (16), 5392-5397.
48. Sedlak, M. *Journal of Chemical Physics* **1994**, 101, (11), 10140-10144.
49. Invitrogen, Molecular Probes.
50. Johnson, C. S. *Progress in Nuclear Magnetic Resonance Spectroscopy* **1999**, 34, (3-4), 203-256.
51. Zero, K.; Ware, B. R. *Journal of Chemical Physics* **1984**, 80, (4), 1610-1616.
52. Yu, K.; Russo, P. S. *Journal of Polymer Science Part B-Polymer Physics* **1996**, 34, (8), 1467-1475.
53. Wang, C. H. *Journal of Chemical Physics* **1991**, 95, (5), 3788-3797.
54. Grabowski, C. A.; Mukhopadhyay, A. *Macromolecules* **2008**, 41, (16), 6191-6194.
55. Schlessinger, J.; Koppel, D. E.; Axelrod, D.; Jacobson, K.; Webb, W. W.; Elson, E. L. *Proceedings of the National Academy of Sciences of the United States of America* **1976**, 73, (7), 2409-2413.
56. Koppel, D. E.; Axelrod, D.; Schlessinger, J.; Elson, E. L.; Webb, W. W. *Biophysical Journal* **1976**, 16, (11), 1315-1329.
57. Kovaleski, J. M.; Wirth, M. J. *Analytical Chemistry* **1997**, 69, (19), A600-A605.

58. Busch, N. A.; Kim, T.; Bloomfield, V. A. *Macromolecules* **2000**, 33, (16), 5932-5937.
59. Wesson, J. A.; Noh, I.; Kitano, T.; Yu, H. *Macromolecules* **1984**, 17, (4), 782-792.
60. Lanni, F.; Ware, B. R. *Review of Scientific Instruments* **1982**, 53, (6), 905-908.
61. Sehgal, A.; Seery, T. A. P. *Macromolecules* **2003**, 36, (26), 10056-10062.
62. Borochoy, N.; Eisenberg, H. *Macromolecules* **1994**, 27, (6), 1440-1445.
63. Iddon, P. D.; Robinson, K. L.; Armes, S. P. *Polymer* **2004**, 45, (3), 759-768.
64. Lepock, J. R.; Thompson, J. E.; Kruuv, J.; Wallach, D. F. H. *Biochemical and Biophysical Research Communications* **1978**, 85, (1), 344-350.
65. Tsarevsky, N. V.; Pintauer, T.; Matyjaszewski, K. *Macromolecules* **2004**, 37, (26), 9768-9778.
66. Brown, J. N.; Hewins, M.; Vanderlinden, J. H. M.; Lynch, R. J. *Journal of Chromatography* **1981**, 204, (JAN), 115-122.

Appendix A: Permissions

For Figure 3.1

Rightslink Printable License

<https://s100.copyright.com/App/PrintableLicenseFrame.jsp?publisher..>

JOHN WILEY AND SONS LICENSE TERMS AND CONDITIONS

Apr 04, 2012

This is a License Agreement between Wayne Huberty ("You") and John Wiley and Sons ("John Wiley and Sons") provided by Copyright Clearance Center ("CCC"). The license consists of your order details, the terms and conditions provided by John Wiley and Sons, and the payment terms and conditions.

All payments must be made in full to CCC. For payment instructions, please see information listed at the bottom of this form.

License Number	2882080385171
License date	Apr 04, 2012
Licensed content publisher	John Wiley and Sons
Licensed content publication	Biopolymers
Licensed content title	Brownian motion of highly charged poly(L-lysine). Effects of salt and polyion concentration
Licensed content author	Sung-Chang Lin, Wylie I. Lee, J. Michael Schurr
Licensed content date	Apr 1, 1978
Start page	1041
End page	1064
Type of use	Dissertation/Thesis
Requestor type	University/Academic
Format	Print and electronic
Portion	Figure/table
Number of figures/tables	1
Number of extracts	
Original Wiley figure/table number(s)	Figure 1
Will you be translating?	No
Order reference number	
Total	0.00 USD

Terms and Conditions

TERMS AND CONDITIONS

This copyrighted material is owned by or exclusively licensed to John Wiley & Sons, Inc. or one of its group companies (each a "Wiley Company") or a society for whom a Wiley Company has exclusive publishing rights in relation to a particular journal (collectively WILEY"). By clicking "accept" in connection with completing this licensing transaction, you agree that the following terms and conditions apply to this transaction (along with the billing and payment terms and conditions established by the Copyright Clearance Center Inc., ("CCC's Billing and Payment terms and conditions"), at the time that you opened your Rightslink account (these are available at any time at <http://myaccount.copyright.com>)

Figure 3.2 and Figure 3.4

Rightslink Printable License

<https://s100.copyright.com/App/PrintableLicenseFrame.jsp?publisher...>

AMERICAN INSTITUTE OF PHYSICS LICENSE TERMS AND CONDITIONS

Apr 13, 2012

All payments must be made in full to CCC. For payment instructions, please see information listed at the bottom of this form.

License Number	2887070986168
Order Date	Apr 13, 2012
Publisher	American Institute of Physics
Publication	Journal of Chemical Physics
Article Title	The ionic strength dependence of the structure and dynamics of polyelectrolyte solutions as seen by light scattering: The slow mode dilemma
Author	Marián Sedláč
Online Publication Date	Dec 8, 1996
Volume number	105
Issue number	22
Type of Use	Thesis/Dissertation
Requestor type	University or Educational Institution
Format	Print and electronic
Portion	Figure/Table
Number of figures/tables	2
Title of your thesis / dissertation	Synthesis of Fluorescent Poly(styrene sulfonate)
Expected completion date	May 2012
Estimated size (number of pages)	66
Total	0.00 USD

Terms and Conditions

American Institute of Physics -- Terms and Conditions: Permissions Uses

American Institute of Physics ("AIP") hereby grants to you the non-exclusive right and license to use and/or distribute the Material according to the use specified in your order, on a one-time basis, for the specified term, with a maximum distribution equal to the number that you have ordered. Any links or other content accompanying the Material are not the subject of this license.

1. You agree to include the following copyright and permission notice with the reproduction of the Material: "Reprinted with permission from [FULL CITATION]. Copyright [PUBLICATION YEAR], American Institute of Physics." For an article, the copyright and permission notice must be printed on the first page of the article or book chapter. For photographs, covers, or tables, the copyright and permission notice may appear with the Material, in a footnote, or in the reference list.
2. If you have licensed reuse of a figure, photograph, cover, or table, it is your responsibility to ensure that the material is original to AIP and does not contain the copyright of another entity, and that the copyright notice of the figure, photograph, cover, or table does not indicate that it was reprinted by AIP, with permission, from

- another source. Under no circumstances does AIP, purport or intend to grant permission to reuse material to which it does not hold copyright.
3. You may not alter or modify the Material in any manner. You may translate the Material into another language only if you have licensed translation rights. You may not use the Material for promotional purposes. AIP reserves all rights not specifically granted herein.
 4. The foregoing license shall not take effect unless and until AIP or its agent, Copyright Clearance Center, receives the Payment in accordance with Copyright Clearance Center Billing and Payment Terms and Conditions, which are incorporated herein by reference.
 5. AIP or the Copyright Clearance Center may, within two business days of granting this license, revoke the license for any reason whatsoever, with a full refund payable to you. Should you violate the terms of this license at any time, AIP, American Institute of Physics, or Copyright Clearance Center may revoke the license with no refund to you. Notice of such revocation will be made using the contact information provided by you. Failure to receive such notice will not nullify the revocation.
 6. AIP makes no representations or warranties with respect to the Material. You agree to indemnify and hold harmless AIP, American Institute of Physics, and their officers, directors, employees or agents from and against any and all claims arising out of your use of the Material other than as specifically authorized herein.
 7. The permission granted herein is personal to you and is not transferable or assignable without the prior written permission of AIP. This license may not be amended except in a writing signed by the party to be charged.
 8. If purchase orders, acknowledgments or check endorsements are issued on any forms containing terms and conditions which are inconsistent with these provisions, such inconsistent terms and conditions shall be of no force and effect. This document, including the CCC Billing and Payment Terms and Conditions, shall be the entire agreement between the parties relating to the subject matter hereof.

This Agreement shall be governed by and construed in accordance with the laws of the State of New York. Both parties hereby submit to the jurisdiction of the courts of New York County for purposes of resolving any disputes that may arise hereunder.

If you would like to pay for this license now, please remit this license along with your payment made payable to "COPYRIGHT CLEARANCE CENTER" otherwise you will be invoiced within 48 hours of the license date. Payment should be in the form of a check or money order referencing your account number and this invoice number RLNK500759904.

Once you receive your invoice for this order, you may pay your invoice by credit card. Please follow instructions provided at that time.

**Make Payment To:
Copyright Clearance Center
Dept 001
P.O. Box 843006
Boston, MA 02284-3006**

For suggestions or comments regarding this order, contact RightsLink Customer Support: customercare@copyright.com or +1-877-622-5543 (toll free in the US) or +1-978-646-2777.

Gratis licenses (referencing \$0 in the Total field) are free. Please retain this printable license for your reference. No payment is required.

Figure 3.3

Rightslink Printable License

<https://s100.copyright.com/App/PrintableLicenseFrame.jsp?publisher...>

AMERICAN INSTITUTE OF PHYSICS LICENSE TERMS AND CONDITIONS

Apr 13, 2012

All payments must be made in full to CCC. For payment instructions, please see information listed at the bottom of this form.

License Number	2887071255025
Order Date	Apr 13, 2012
Publisher	American Institute of Physics
Publication	Journal of Chemical Physics
Article Title	Dynamics of moderately concentrated salt-free polyelectrolyte solutions: Molecular weight dependence
Author	Marián Sedláč, Eric J. Amis
Online Publication Date	Jan 1, 1992
Volume number	96
Issue number	1
Type of Use	Thesis/Dissertation
Requestor type	University or Educational Institution
Format	Print and electronic
Portion	Figure/Table
Number of figures/tables	1
Title of your thesis / dissertation	Synthesis of Fluorescent Poly(styrene sulfonate)
Expected completion date	May 2012
Estimated size (number of pages)	66
Total	0.00 USD

Terms and Conditions

American Institute of Physics -- Terms and Conditions: Permissions Uses

American Institute of Physics ("AIP") hereby grants to you the non-exclusive right and license to use and/or distribute the Material according to the use specified in your order, on a one-time basis, for the specified term, with a maximum distribution equal to the number that you have ordered. Any links or other content accompanying the Material are not the subject of this license.

1. You agree to include the following copyright and permission notice with the reproduction of the Material: "Reprinted with permission from [FULL CITATION]. Copyright [PUBLICATION YEAR], American Institute of Physics." For an article, the copyright and permission notice must be printed on the first page of the article or book chapter. For photographs, covers, or tables, the copyright and permission notice may appear with the Material, in a footnote, or in the reference list.
2. If you have licensed reuse of a figure, photograph, cover, or table, it is your responsibility to ensure that the material is original to AIP and does not contain the copyright of another entity, and that the copyright notice of the figure, photograph, cover, or table does not indicate that it was reprinted by AIP, with permission, from another source. Under no circumstances does AIP, purport or intend to grant

- permission to reuse material to which it does not hold copyright.
3. You may not alter or modify the Material in any manner. You may translate the Material into another language only if you have licensed translation rights. You may not use the Material for promotional purposes. AIP reserves all rights not specifically granted herein.
 4. The foregoing license shall not take effect unless and until AIP or its agent, Copyright Clearance Center, receives the Payment in accordance with Copyright Clearance Center Billing and Payment Terms and Conditions, which are incorporated herein by reference.
 5. AIP or the Copyright Clearance Center may, within two business days of granting this license, revoke the license for any reason whatsoever, with a full refund payable to you. Should you violate the terms of this license at any time, AIP, American Institute of Physics, or Copyright Clearance Center may revoke the license with no refund to you. Notice of such revocation will be made using the contact information provided by you. Failure to receive such notice will not nullify the revocation.
 6. AIP makes no representations or warranties with respect to the Material. You agree to indemnify and hold harmless AIP, American Institute of Physics, and their officers, directors, employees or agents from and against any and all claims arising out of your use of the Material other than as specifically authorized herein.
 7. The permission granted herein is personal to you and is not transferable or assignable without the prior written permission of AIP. This license may not be amended except in a writing signed by the party to be charged.
 8. If purchase orders, acknowledgments or check endorsements are issued on any forms containing terms and conditions which are inconsistent with these provisions, such inconsistent terms and conditions shall be of no force and effect. This document, including the CCC Billing and Payment Terms and Conditions, shall be the entire agreement between the parties relating to the subject matter hereof.

This Agreement shall be governed by and construed in accordance with the laws of the State of New York. Both parties hereby submit to the jurisdiction of the courts of New York County for purposes of resolving any disputes that may arise hereunder.

If you would like to pay for this license now, please remit this license along with your payment made payable to "COPYRIGHT CLEARANCE CENTER" otherwise you will be invoiced within 48 hours of the license date. Payment should be in the form of a check or money order referencing your account number and this invoice number RLNK500759913.

Once you receive your invoice for this order, you may pay your invoice by credit card. Please follow instructions provided at that time.

**Make Payment To:
Copyright Clearance Center
Dept 001
P.O. Box 843006
Boston, MA 02284-3006**

For suggestions or comments regarding this order, contact RightsLink Customer Support: customer@copyright.com or +1-877-622-5543 (toll free in the US) or +1-978-646-2777.

Gratis licenses (referencing \$0 in the Total field) are free. Please retain this printable license for your reference. No payment is required.

For Figure 3.5



RightsLink®

Home

Account
Info

Help



ACS Publications
High quality. High impact.

Title: Light scattering by dilute solutions of salt-free polyelectrolytes
Author: Maurice Drifford et al.
Publication: The Journal of Physical Chemistry B
Publisher: American Chemical Society
Date: Oct 1, 1984
Copyright © 1984, American Chemical Society

Logged in as:
Wayne Huberty

LOGOUT

PERMISSION/LICENSE IS GRANTED FOR YOUR ORDER AT NO CHARGE

This type of permission/license, instead of the standard Terms & Conditions, is sent to you because no fee is being charged for your order. Please note the following:

- Permission is granted for your request in both print and electronic formats.
- If figures and/or tables were requested, they may be adapted or used in part.
- Please print this page for your records and send a copy of it to your publisher/graduate school.
- Appropriate credit for the requested material should be given as follows: "Reprinted (adapted) with permission from (COMPLETE REFERENCE CITATION). Copyright (YEAR) American Chemical Society." Insert appropriate information in place of the capitalized words.
- One-time permission is granted only for the use specified in your request. No additional uses are granted (such as derivative works or other editions). For any other uses, please submit a new request.

BACK

CLOSE WINDOW

Copyright © 2012 Copyright Clearance Center, Inc. All Rights Reserved. [Privacy statement](#).
Comments? We would like to hear from you. E-mail us at customercare@copyright.com

For Figure 4.1 and Figure 4.2

Rightslink Printable License

<https://s100.copyright.com/App/PrintableLicenseFrame.jsp?publisher...>

SPRINGER LICENSE TERMS AND CONDITIONS

Apr 13, 2012

This is a License Agreement between Wayne Huberty ("You") and Springer ("Springer") provided by Copyright Clearance Center ("CCC"). The license consists of your order details, the terms and conditions provided by Springer, and the payment terms and conditions.

All payments must be made in full to CCC. For payment instructions, please see information listed at the bottom of this form.

License Number	2887080575880
License date	Apr 13, 2012
Licensed content publisher	Springer
Licensed content publication	Springer eBook
Licensed content title	Fluorescence Photobleaching Recovery
Licensed content author	P. S. Russo
Licensed content date	Dec 1, 2008
Type of Use	Thesis/Dissertation
Portion	Figures
Author of this Springer article	No
Order reference number	
Title of your thesis / dissertation	Synthesis of Fluorescent Poly(styrene sulfonate)
Expected completion date	May 2012
Estimated size(pages)	66
Total	0.00 USD
Terms and Conditions	

Introduction

The publisher for this copyrighted material is Springer Science + Business Media. By clicking "accept" in connection with completing this licensing transaction, you agree that the following terms and conditions apply to this transaction (along with the Billing and Payment terms and conditions established by Copyright Clearance Center, Inc. ("CCC"), at the time that you opened your Rightslink account and that are available at any time at <http://myaccount.copyright.com>).

Limited License

With reference to your request to reprint in your thesis material on which Springer Science and Business Media control the copyright, permission is granted, free of charge, for the use indicated in your enquiry.

Licenses are for one-time use only with a maximum distribution equal to the number that

you identified in the licensing process.

This License includes use in an electronic form, provided its password protected or on the university's intranet or repository, including UMI (according to the definition at the Sherpa website: <http://www.sherpa.ac.uk/romeo/>). For any other electronic use, please contact Springer at (permissions.dordrecht@springer.com or permissions.heidelberg@springer.com).

The material can only be used for the purpose of defending your thesis, and with a maximum of 100 extra copies in paper.

Although Springer holds copyright to the material and is entitled to negotiate on rights, this license is only valid, provided permission is also obtained from the (co) author (address is given with the article/chapter) and provided it concerns original material which does not carry references to other sources (if material in question appears with credit to another source, authorization from that source is required as well).

Permission free of charge on this occasion does not prejudice any rights we might have to charge for reproduction of our copyrighted material in the future.

Altering/Modifying Material: Not Permitted

You may not alter or modify the material in any manner. Abbreviations, additions, deletions and/or any other alterations shall be made only with prior written authorization of the author(s) and/or Springer Science + Business Media. (Please contact Springer at (permissions.dordrecht@springer.com or permissions.heidelberg@springer.com))

Reservation of Rights

Springer Science + Business Media reserves all rights not specifically granted in the combination of (i) the license details provided by you and accepted in the course of this licensing transaction, (ii) these terms and conditions and (iii) CCC's Billing and Payment terms and conditions.

Copyright Notice:Disclaimer

You must include the following copyright and permission notice in connection with any reproduction of the licensed material: "Springer and the original publisher /journal title, volume, year of publication, page, chapter/article title, name(s) of author(s), figure number(s), original copyright notice) is given to the publication in which the material was originally published, by adding: with kind permission from Springer Science and Business Media"

Warranties: None

Example 1: Springer Science + Business Media makes no representations or warranties with respect to the licensed material.

Example 2: Springer Science + Business Media makes no representations or warranties with respect to the licensed material and adopts on its own behalf the limitations and disclaimers established by CCC on its behalf in its Billing and Payment terms and conditions for this licensing transaction.

Indemnity

You hereby indemnify and agree to hold harmless Springer Science + Business Media and CCC, and their respective officers, directors, employees and agents, from and against any and all claims arising out of your use of the licensed material other than as specifically authorized pursuant to this license.

No Transfer of License

This license is personal to you and may not be sublicensed, assigned, or transferred by you to any other person without Springer Science + Business Media's written permission.

No Amendment Except in Writing

This license may not be amended except in a writing signed by both parties (or, in the case of Springer Science + Business Media, by CCC on Springer Science + Business Media's behalf).

Objection to Contrary Terms

Springer Science + Business Media hereby objects to any terms contained in any purchase order, acknowledgment, check endorsement or other writing prepared by you, which terms are inconsistent with these terms and conditions or CCC's Billing and Payment terms and conditions. These terms and conditions, together with CCC's Billing and Payment terms and conditions (which are incorporated herein), comprise the entire agreement between you and Springer Science + Business Media (and CCC) concerning this licensing transaction. In the event of any conflict between your obligations established by these terms and conditions and those established by CCC's Billing and Payment terms and conditions, these terms and conditions shall control.

Jurisdiction

All disputes that may arise in connection with this present License, or the breach thereof, shall be settled exclusively by arbitration, to be held in The Netherlands, in accordance with Dutch law, and to be conducted under the Rules of the 'Netherlands Arbitrage Instituut' (Netherlands Institute of Arbitration). **OR:**

All disputes that may arise in connection with this present License, or the breach thereof, shall be settled exclusively by arbitration, to be held in the Federal Republic of Germany, in accordance with German law.

Other terms and conditions:

v1.3

If you would like to pay for this license now, please remit this license along with your payment made payable to "COPYRIGHT CLEARANCE CENTER" otherwise you will be invoiced within 48 hours of the license date. Payment should be in the form of a check or money order referencing your account number and this invoice number RLNK500759926.

Once you receive your invoice for this order, you may pay your invoice by credit card. Please follow instructions provided at that time.

**Make Payment To:
Copyright Clearance Center
Dept 001
P.O. Box 843006
Boston, MA 02284-3006**

Appendix B: List of Abbreviations and Symbols

CHCA	α -cyano-4-hydroxycinnamic acid
2 EXP	2 exponential fit
AUC	Analytical ultracentrifugation
Å	Angstrom
N_a	Avogadro's number
B	Bjerrum length
k_B	Boltzmann's constant
$^{\circ}\text{C}$	Celsius
cm	Centimeters
$f(A)$	Coherence parameter
c_p	Concentration of polymer
c_s	Concentration of salt
DNA	Deoxyribonucleic acid
DLS	Dynamic light scattering
FITC	Fluorescein isothiocyanate isomer 1
FCS	Fluorescence correlation spectroscopy
FPR	Fluorescence photobleaching recovery
$P(\theta)$	Form factor
GPC	Gel permeation chromatography
GPC/MALLS	Gel permeation chromatography with multi-angle laser light scattering
R_h	Hydrodynamic radius

I	Ionic strength
K	Kelvin
m/z	Mass to charge ratio
MALDI	Matrix assisted laser desorption ionization
MHz	Megahertz
μL	Microliter
mL	Milliliter
min	Minutes
M	Molar
mol	Mole
M	Molecular weight
N_2	Nitrogen
ν	Number density
\bar{v}_1	Partial molar volume
NaPSS	Polystyrene sulfonate
PDI	Polydispersity index
$^1\text{H NMR}$	Proton nuclear magnetic resonance spectroscopy
DOSY	Pulsed field gradient NMR spectroscopy
R_g	Radius of gyration
\mathcal{R}	Rayleigh factor
q	Scattering vector
s	Seconds
SAXS	Small angle scattering

η_o	Solvent viscosity
SLS	Static light scattering
T	Temperature

Vita

Wayne Huberty was born in Colorado Springs in 1985. He grew up in Appleton Wisconsin and graduated high school in 2004. He attended a small state school, University of Wisconsin-Stevens Point and obtained the Bachelor of Science in Chemistry and Biology. In the fall of 2009, he started work towards a master's degree in chemistry in May 2012.